Contrib Mineral Petrol (2006) 152:721–742
DOI 10.1007/s00410-006-0129-9

ORIGINAL PAPER

The petrogenesis of Carboniferous–Permian dyke and sill intrusions across northern Europe

L. A. Kirstein · G. R. Davies · M. Heeremans

Received: 8 February 2006 / Accepted: 26 July 2006 / Published online: 29 August 2006
© Springer-Verlag 2006

Abstract The presence or absence of a thermally anomalous mantle plume during the formation of the widespread Carboniferous–Permian magmatism of northern Europe is examined. The geochemistry of representative samples from the extensive Carboniferous–Permian dyke and sill intrusions across northern Europe are reported in order to ascertain whether they have a common 'plume' source. Both tholeiitic and alkaline magmas have diverse trace element compositions. Alkaline samples with relatively low Ti and Nb/La < 1 are considered to originate in the lithospheric mantle and those with Nb/La > 1 from the asthenosphere. The tholeiites have a close affinity to E-MORB but have mixed with variable amounts of lithosphere and upper crust. Tectonic reorganisation and decompression melting of a trace element-enriched mantle is considered to have controlled the Carboniferous–Permian magmatism, which contains no coherent geochemical evidence for a single plume-related thermo-chemical anomaly.

Communicated by I. Parsons.

L. A. Kirstein (✉)
Grant Institute of Earth Science, University of Edinburgh,
West Mains Road, Edinburgh EH9 3JW, UK
e-mail: linda.kirstein@ed.ac.uk

G. R. Davies
Faculty of Earth and Life Sciences, Vrije Universiteit,
1085 De Boelelaan, 1081 HV Amsterdam, The Netherlands

M. Heeremans
Department of Geology, University of Oslo,
P.O. Box 1047, Blindern, 0316 Oslo, Norway

Introduction

Carboniferous–Permian magmatism is widespread across Europe from the British Isles to the Baltic Sea and south to the Iberian Peninsula. The estimated volume of extruded and intruded magmatic products in Norway and Scotland is approximately 35,000 km^3, more than 80% of which occurs in Norway (Tomkeieff 1937; Ramberg and Larsen 1978; Neumann et al. 2004). Much of this material was generated in two main pulses of activity each lasting approximately 5 million years at 340 and 295 Ma (Timmerman 2004). In this contribution we consider the regionally extensive intrusive dykes and sills from the area north of the Variscan orogenic front and investigate the regional chemical variations in terms of different sources, lithospheric thickness variation and the role of volatiles. The combined Carboniferous–Permian dyke swarms and sills are prominent features of geological and geophysical maps extending from the British Isles across the North Sea and throughout Scandinavia (Fig. 1). The orientation of the dykes from NE–SW and E–W in Britain, to N–S in the Oslo Graben and NW–SE in Scania, southern Sweden, has been used to suggest the presence of a mantle plume at the position of intersection (Ernst and Buchan 1997). Chemical and tectonic evidence for such a plume, however, remains limited and requires further examination.

Some of the intrusions are associated with lavas, but, a distinct majority (approximately 60%) have no obvious associated lavas. The intrusions can be divided into different groups on the basis of geochronology and geochemistry. The quartz tholeiitic dyke and sill intrusions from across the region, including borehole material from the North Sea, have been shown to be

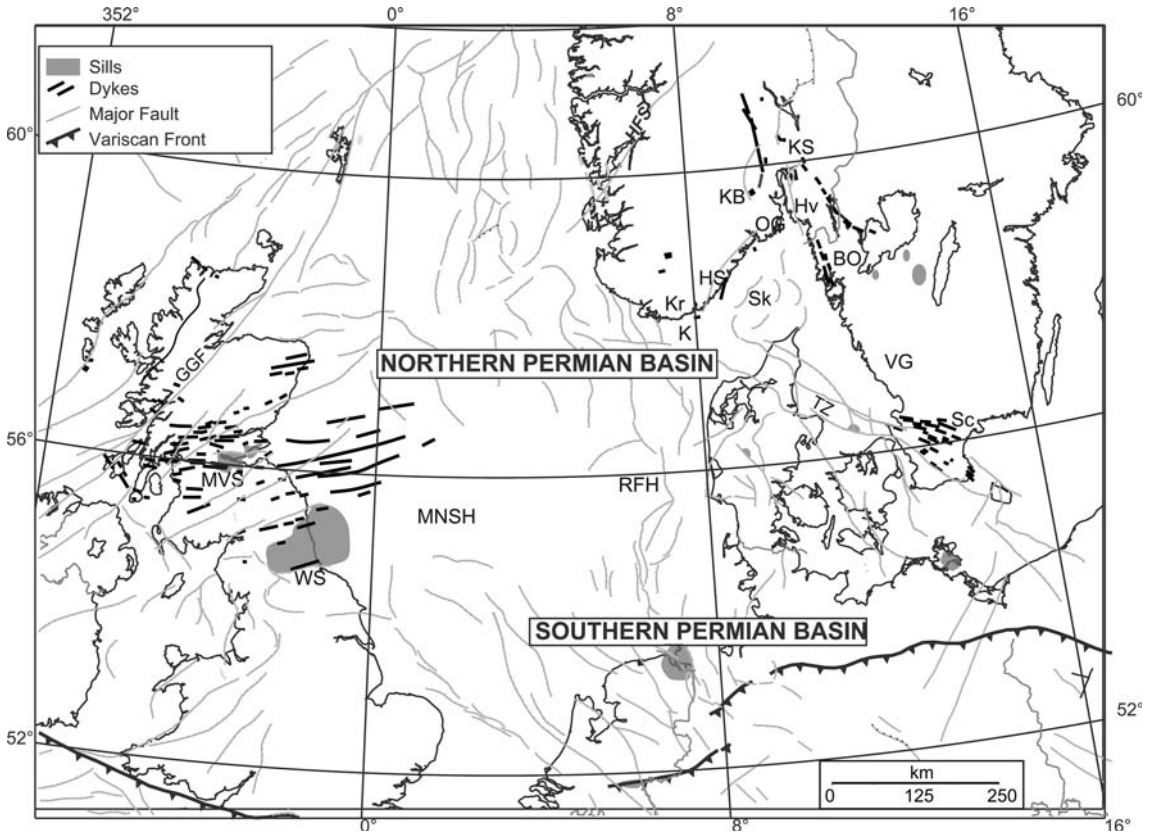

Fig. 1 Map of northern Europe highlighting the major structural features including the Skaggerak Graben (*Sk*) and the extensive Carboniferous–Permian dyke and sill intrusions. *GGF* Great Glen Fault; *MVS* Midland Valley sill; *WS* Whin Sill; *MNSH* Mid North Sea High; *RFH* Ringkøbing-Fyn High; *K* Kattegat; *TZ* Tornquist Zone; *Sc* Scania; *VG* Västergötland; *BO* Bohüslan; *OG* Oslo Graben; *KB* Kongsberg; *Kr* Kristiansand; *KS* Kroksk-ogen; *Hv* Hovedøya island; *HS* Hisøy

broadly contemporaneous at 295 Ma (DeSouza 1982; Timmerman 2004). The overall range in the ages of the various alkaline to tholeiitic intrusions is, however, much greater, spanning a period of 80 million years from early Carboniferous (340 Ma) to early Permian (260 Ma). To date comparative studies of the chemical compositions of the dykes and sills from across northern Europe that span the 80 million year age range have been relatively limited in geographic coverage (Neumann et al. 2004). In an attempt to constrain relationships between the regional magmatism and assess the possible involvement of a thermal anomaly, an extensive geochemical study was undertaken of samples from Scotland, England, Norway and Sweden.

Tectonic setting

The Carboniferous–Permian marked a period of tectonic change across northern Europe. Carboniferous–Permian development is characterized by three main tectonic and/or magmatic events: (1) the development of the West European Carboniferous Basin (see Maynard et al. 1997); (2) a period of basaltic volcanism during the late Carboniferous–early Permian (Lower Rotliegend); and (3) the development of the Northern and Southern Permian Basins in late Permian times (Upper Rotliegend; see, e.g. Ziegler 1990; Glennie 1998).

The development of the West European Carboniferous Basin, stretching from Great Britain to Poland, started with the formation of early Carboniferous grabens north of the Variscan subduction front (Leeder 1982; Maynard et al. 1997). Closure of the Rhenohercynian ocean and concomitant deformation in the Rhenohercynian fold-and-thrust belt occurred in Namurian times (333–318 Ma, Maynard et al. 1997). Foreland basins developed across north-west Europe during the late Carboniferous (McCann 1999) and experienced inversion tectonics due to ongoing Variscan deformation to the south (e.g. Corfield et al. 1996; Maynard et al. 1997). The emplacement of dykes and sills during the late Carboniferous–early Permian marks a change from foreland basin development to a more widespread thermal and extensional event. Sizeable volumes of tholeiitic basalts were extruded or

emplaced over large parts of Europe at *c.* 300–295 Ma (see e.g. Neumann et al. 2004; Timmerman 2004) possibly implying the involvement of a plume-related thermal anomaly. Following this magmatic event, the North Sea remained an area of non-deposition until the late Permian, when continental sediments were deposited in the rapidly evolving Southern and Northern Permian Basins. These basins were separated by the discontinuous Mid-North Sea High and the Ringkøbing-Fyn High (Fig. 1).

Description of the intrusions

UK—Scotland and northern England

The dykes of Carboniferous–Permian age in Scotland alone number ≥3,000, stretching from the Midland Valley of Scotland to the Scottish Highlands and Islands (Rock 1983) (Fig. 1). A number of exceedingly large sill complexes, including the Midland Valley and the Whin Sill, are also preserved (Fig. 1). The field characteristics and petrography of these intrusions have been described in detail elsewhere (Walker 1935; Macdonald et al. 1981; Rock 1983; Upton et al. 2004).

The intrusions can be divided into a number of different petrographic types including alkaline lamprophyres, olivine nephelinites, olivine dolerites, quartz dolerites and more felsic microsyenites. The alkaline dykes are prolific, generally <1 m wide and vary from aphyric to porphyritic, containing occasional ultramafic and crustal xenoliths. From cross-cutting relationships and high precision dating it is evident that there are at least two phases of alkaline dyke intrusion (Baxter and Mitchell 1984; Monaghan and Pringle 2004). The first occurred in the Visean-Westphalian (340–300 Ma) and the second during the Permian (290–248 Ma); the latter are primarily concentrated in northern Scotland (Timmerman 2004). Extrusive equivalents are not preserved in the Scottish Highlands (Francis 1991), although extrusive equivalents of alkaline lavas are preserved in the Mauchline Basin in Ayrshire (De Souza 1982). Alkali dolerite sills are also common and associated with the numerous surface vents that are distributed across Scotland and especially along the east coast (Upton et al. 2004). These sills are considered co-magmatic with extrusive, particularly pyroclastic rocks (Francis 1991).

The quartz tholeiite intrusions are late Carboniferous in age (295 ± 5 Ma) (Timmerman 2004; Monaghan and Pringle 2004). Dykes range in width up to 50 m, averaging 30 m, trend WNW–ENE, and continue offshore for more than 200 km (Smythe 1994). These dykes record evidence of marked late stage differentiation with rapidly cooled aphyric margins that grade into porphyritic centres (Macdonald et al. 1981). The silica-oversaturated tholeiitic dykes are associated with contemporaneous major sills, including the Midland Valley complex of Scotland and the Whin Sill complex of northern England. These sill complexes are dated at 295 ± 3 Ma (Timmerman 2004). Individual sills can attain thicknesses of ~200 m (Macdonald et al. 1981), and have no known extrusive equivalents (Francis 1991).

Norway

Dykes are widespread along the coast of Norway from Magerøy in the north to Kristiansand in the south, with a concentration in the region around the Oslo Graben (Fig. 1). The north-western coastal dykes are related to early Carboniferous rifting in the Barents Sea (Løvlie and Mitchell 1982). Younger dykes intruded along the west coast during the Permian are closely associated with the development of the North Sea Basin. Therefore it is primarily dykes and sills intruded along the south coast and close to the Oslo Graben that are potentially associated with a plume influence on Carboniferous–Permian magmatism. Activity in the Oslo region was episodic and extended over approximately 50 million years, from late Carboniferous (300 Ma) to late Permian/early Triassic (248 Ma) (Sundvoll et al. 1990; Neumann et al. 1992; 2004). The dykes and sills commonly intrude Palaeozoic sediments and in some cases are clearly offset, often by up to 1 m, by late-stage Carboniferous–Permian faulting. The compositions of the dykes vary from mafic to felsic and include alkaline, tholeiitic and felsic intrusions. Despite recent improved chronology and the cross cutting relationships, it is difficult to constrain the exact temporal relationship between the different generations of dykes and sills.

The tholeiitic dykes trend NE–SW and are dated at 295 ± 5 Ma. They are contemporaneous with the oldest alkaline intrusion (298.6 ± 1.4 Ma) (Dahlgren et al. 1996) and appear synchronous with the major period of lava eruption associated with initial rift development in the Oslo Graben (Sundvoll et al. 1990; Neumann et al. 2004). The timing of dyke emplacement relative to the earliest alkaline sills is uncertain. However, it has been suggested that the microsyenite sills and tholeiitic dykes were emplaced in a similar time interval (Timmerman 2004). These microsyenites are often crosscut by a set of E–W trending intermediate dykes, which in turn are crosscut by compositionally similar dykes that are N–S trending. A NE–SW trend is evident in the felsic intrusions, which are crosscut by more

basic alkaline dykes. The rhomb porphyry (RP–trachyandesite with large feldspar rhombs) dykes and sills are extensive and constitute a large volume of the volcanic material in the Oslo Graben. Evidence that basic alkaline magmatism continued throughout most of the magmatic history of the Oslo Graben is provided by fragmented blocks of RP in a large basic dyke on Hovedøya Island, in the Oslo Fjord (Fig. 1). Occasional alkaline basaltic lavas are also found within the RP lava series and basaltic lavas occur in the central volcanoes that represent a relatively late stage in the rift history. In a recent Ar–Ar study by Timmerman (unpublished data) two later phases of alkaline activity were recorded in the mid Permian (~270 Ma) and late Permian (~250 Ma). The older, mid Permian age is consistent with ages derived for the youngest larvikite and monzonite intrusions in the Oslo Graben (Pederson et al. 1995).

The alkaline dykes are thin (< 1 m), numerous and are observed to be often offset in an *en echelon* manner with fractured margins. Some dykes, particularly close to the Oslo Graben axis, contain crustal xenoliths up to 40 cm in diameter with compositions including granulite and gneiss. The dykes commonly contain plagioclase feldspar, Ti-rich amphibole, Ti-rich salite, diopside and biotite, which is unusually Ti-rich (Scott and Middleton 1983).

Tholeiite dykes are thicker (>1 m), as are the RP dykes (generally <15 m, but up to 50 m wide south east of the Oslo Graben) that have equivalent lavas. Larger tholeiite dykes show compositional variations from margins to core with the core regions commonly containing up to 40% phenocrysts, primarily plagioclase feldspar, pyroxene and iron oxides. The margins are relatively aphyric with recognisable flow margins. RP contain both alkali and plagioclase feldspar, with alkali feldspar phenocrysts up to 5 cm.

Sills tend to be thin (~20 m thick), and are classed as microsyenites, alkali basalts and dolerites, with the former dominant at the beginning and very end of the intrusive magmatic event(s). The sills and dykes contain feldspar ± olivine ± pyroxene ± amphibole ± biotite. Accessory apatite, up to 0.8 mm long, occurs both in the early microsyenites and late stage RP and syenites. Additional accessory minerals include REE-rich carbonates such as parisite and synchisite, as well as zircon, which makes up to 2% of the mode, especially in the microsyenites.

Sweden

Intrusions in Sweden are most evident on the eastern edge of the Oslo Graben along the Skagerrak coast, with a major concentration in Scania, southern Sweden (Fig. 1). Both alkaline and tholeiitic intrusions occur in Bohüslan and Västergötland and are widespread in Scania (Bylund et al. 1988). No lavas are preserved in the region. The Scania dykes that intrude PreCambrian and Palaeozoic strata, all trend NW–SE parallel to the Tornquist zone, while those along the Skagerrak coast trend N–S or NNW–SSE. Alkaline dykes are less than 1.5 m wide, contain occasional crustal xenoliths and are commonly fractured. Syenite and RP intrusions between 5 and 50 m wide also occur (Samuelsson 1971). The RP in Sweden have been related to the RP lavas in the Oslo region (Samuelsson 1971; Kresten et al. 1981). In Scania the majority of the dykes and sills were intruded in the late Carboniferous (295 ± 10 Ma) (Klingspor 1976; Obst et al. 2004; Timmerman 2004). Sill emplacement in central Sweden was contemporaneous with that in Scania (Timmerman 2004).

Summary

Igneous activity was episodic, with short periods of activity punctuated by large spells of inactivity in all regions. In Scotland, activity ranged from the early Carboniferous (340 Ma) to Upper Permian (~260 Ma). Elsewhere magmatism commenced later. The earliest Skien lavas in the Oslo Graben are dated at ~300 Ma (Sundvoll et al. 1990), although recent dating suggests that activity in these regions continued until latest Permian or early Triassic (M.J. Timmerman, personal communication). A more detailed discussion of the timing and relative volume of Carboniferous–Permian magmatism can be found in Wilson et al. 2004. A large tholeiitic event is recorded across northern Europe at about 295 Ma. Whether magmatism across this broad area is related remains to be demonstrated but is key to hypotheses regarding the presence of a mantle plume in Northern Europe during the Carboniferous–Permian.

Methods

Over 70 samples from the UK, Norway and Sweden have been analysed by X-ray fluorescence (XRF) for major and trace element abundances. Sample locations are given in Appendix 3. A subset (43) of the samples was also analysed by inductively coupled plasma mass spectrometry (ICPMS) for additional trace elements. Representative analyses are given in Tables 1, 2 and 3; the remaining data are in Appendix 1. The XRF analyses were carried out at the Vrije Universiteit, Amsterdam while the ICPMS data were collected at

Boston University, USA. The analytical details and error analyses are given in the table footnotes and Appendix 2.

Alteration

Post-emplacement alteration and weathering of some Carboniferous–Permian samples was apparent in the field. Thin sections of all apparently fresh samples were examined and further petrographic screening was carried out prior to geochemical analysis. The freshest samples were thus selected but fresh olivine is extremely rare and variable pyroxene and feldspar breakdown is evident in the majority of samples.

Loss on ignition (LOI) values can be used in some instances as a proxy for secondary alteration, although iron oxidation has the opposite effect on LOI values to volatile loss. LOI values were determined on all samples (Tables 1, 2). It is evident from the data tables that several of the alkaline samples have high LOI values, between 2 and 5% on average, and mobile elements such as K_2O and P_2O_5 show more scatter than TiO_2 for example (Tables 1, 2). The major element data have not been recalculated to 100% to avoid introducing skew to the data set. Although alteration is a concern, the following interpretation and petrogenetic discussion is focussed on the least mobile incompatible elements making us confident in our conclusions.

Major element variations

The samples were classified initially using major elements with respect to the alkaline and tholeiitic fields in Fig. 2. However, ratios of relatively immobile elements have been used (e.g. Nb/Y, Zr/Nb) also in light of the LOI values measured. Tholeiites are characterised by having Nb/Y < 0.6 and Zr/Nb > 9.5 (Winchester and Floyd 1977). The trace element ratios suggest that alteration has led to the displacement of certain samples from the fields in which they originally crystallised. The affected samples are clearly identified in Fig. 2 and Table 1. It was primarily the low SiO_2 samples from Norway that were reclassified from alkaline to tholeiitic on the basis of the trace elements.

The samples define a large compositional range with all geographical areas including both alkaline and tholeiitic rocks. The samples appear to be the intrusive equivalents of basalts, basanites, trachybasalts, basaltic trachyandesites and trachytes. It is evident from Fig. 2 that there are marked variations in chemical composition in all areas. The majority of dykes and sills analysed from Scotland are tholeiites, although a number of alkaline intrusions have also been sampled. All are mafic (<52 wt% SiO_2) in composition.

Over 40 dykes and sills were analysed from southern Norway of which there is an approximately equal distribution of mafic and felsic intrusions. Of the mafic intrusions very few are tholeiitic. The tholeiites sampled are located on the island of Hisøy and near Kongsberg (Fig. 1). A comparable low proportion of tholeiite compositions is found in the lavas of the Oslo Graben (Neumann et al. 2004). The small number of tholeiitic dykes in southern Norway is therefore considered to reflect the true distribution of tholeiitic intrusions and not a sampling bias. Within the entire dataset, the Norwegian samples show the greatest chemical diversity including samples with up to 70 wt% SiO_2. All samples from southern Sweden are

Table 1 Selected major and trace element data analysed by XRF from tholeiite intrusions

Sample	Country	Type	SiO_2	TiO_2	Al_2O_3	Fe_2O_3	MnO	MgO	CaO	Na_2O	K_2O	P_2O_5	LOI	Total	Rb	Sr	Y	Zr	Nb	V	Ni
ARN-1	Scotland	Sill	49.51	1.96	13.56	12.82	0.17	6.81	8.00	3.41	1.63	0.23	2.00	100.2	30	340	25	135	13	302	82
DCW-1	Scotland	Dyke	48.46	2.68	13.74	13.71	0.19	6.46	9.77	2.21	0.58	0.27	1.30	99.4	13	316	30	171	18	373	97
LC-3	Scotland	Sill	49.86	2.16	13.80	13.10	0.18	6.16	7.28	3.25	1.70	0.27	1.90	99.7	38	474	29	166	15	322	65
MdC-1	Scotland	Dyke	49.98	2.46	13.62	13.83	0.22	6.00	9.59	2.36	0.65	0.24	0.70	99.7	16	291	33	175	18	372	77
LC-1	Scotland	Dyke	50.06	3.18	13.02	14.71	0.17	5.26	5.49	3.19	1.85	0.60	2.30	99.9	44	492	42	268	23	310	18
PW-1	Scotland	Sill	47.69	2.45	13.92	14.46	0.14	4.64	6.79	3.26	0.57	0.32	5.60	99.8	42	42	29	175	16	338	60
[a]Hy-4	Norway	Dyke	43.62	2.81	14.13	14.65	0.23	6.19	9.81	3.18	0.76	0.22	3.60	99.2	16	393	26	126	11	473	71
[a]Hy-1	Norway	Dyke	44.02	3.13	14.06	14.84	0.23	5.11	9.85	2.85	0.31	0.32	4.50	99.3	4	471	30	155	14	470	31
[a]Hy-2	Norway	Dyke	43.92	3.02	12.97	15.19	0.24	4.99	10.89	2.44	0.42	0.45	4.40	98.9	6	332	37	169	13	501	46
KB-1	Norway	Dyke	51.80	2.22	13.43	13.41	0.18	4.73	8.08	3.02	1.39	0.29	1.00	99.7	42	315	39	219	18	332	57
BIL 1	Sweden	Sill	48.84	1.83	14.92	12.98	0.17	7.53	9.93	2.55	0.45	0.16	0.57	99.9	9	363	21	86	9	248	77
D2	Sweden	Dyke	49.84	2.10	13.82	12.79	0.18	6.68	9.99	2.33	0.83	0.20	1.10	99.9	38	303	27	141	14	322	101
ML-1	Sweden	Dyke	52.34	2.23	13.44	13.56	0.19	4.80	8.10	3.02	1.39	0.28	0.90	100.4	41	318	39	219	18	326	56

Estimated relative accuracy due to calibration errors ± 1%. Total Fe as Fe_2O_3. Samples arranged by location and ordered by decreasing MgO content

[a] Indicates major and trace elements used in defining category

Table 2 Selected major and trace element data analysed by XRF from alkaline intrusions

Sample	Country	Type	SiO_2	TiO_2	Al_2O_3	Fe_2O_3	MnO	MgO	CaO	Na_2O	K_2O	P_2O_5	LOI	Total	Rb	Sr	Y	Zr	Nb	V	Ni
CK-1	Scotland	Sill	45.21	1.54	13.07	11.71	0.17	11.83	9.75	2.96	1.60	0.35	1.50	99.7	39	553	20	144	39	232	272
Hh-1	Scotland	Sill	45.52	1.50	13.47	12.71	0.18	11.73	9.64	2.92	1.06	0.25	0.40	99.5	25	451	20	105	24	230	284
Stc-4	Scotland	Dyke	40.34	2.93	11.89	13.26	0.27	10.76	11.37	0.91	2.33	0.79	4.10	99.1	65	1360	26	276	85	270	325
Moy5	Scotland	Dyke	37.35	2.76	10.58	12.42	0.16	9.00	8.88	1.83	1.60	0.52	13.70	98.9	42	728	23	279	46	264	309
A7ii	Scotland	Dyke	44.89	2.62	13.35	11.29	0.15	7.00	9.25	2.62	1.91	0.63	5.70	99.4	38	699	25	344	55	203	156
NB-1	Scotland	Sill	50.50	2.46	15.53	10.10	0.17	2.96	5.95	4.90	2.94	0.85	3.20	99.7	80	506	44	374	80	103	6
TK-1	Sweden	Dyke	42.76	1.31	13.92	10.35	0.20	10.25	12.28	2.28	1.49	0.74	3.70	99.4	71	775	28	186	81	290	196
HV2	Sweden	Dyke	47.85	2.78	15.20	12.63	0.17	5.63	9.45	3.10	0.99	0.63	1.30	99.8	16	619	33	218	36	335	94
HV1	Sweden	Dyke	47.14	3.46	13.40	13.93	0.22	5.11	7.77	4.27	1.39	0.87	1.50	99.1	63	380	46	266	43	430	48
Al-1	Sweden	Dyke	47.10	2.65	16.41	12.09	0.14	4.90	9.44	3.24	1.26	0.57	1.80	99.7	37	718	30	182	31	328	64
M1	Sweden	Sill	45.69	2.68	15.76	12.59	0.16	4.89	8.01	3.23	0.95	0.39	4.70	99.1	28	547	26	213	27	330	40
VB2	Sweden	Dyke	52.03	2.51	16.05	10.34	0.16	3.41	6.16	4.16	2.79	0.64	1.20	99.5	91	573	48	584	98	218	36
HvS1	Sweden	Dyke	51.76	2.51	15.85	10.34	0.16	3.40	6.04	4.12	2.90	0.64	1.20	99.0	94	588	48	581	96	220	36
JN-1	Norway	Sill	41.01	2.84	9.84	12.74	0.16	11.18	13.18	1.54	0.75	0.20	5.30	98.8	18	649	20	142	30	457	138
Vo-1	Norway	Dyke	44.84	2.19	16.04	9.51	0.15	7.80	8.37	2.48	2.20	0.55	4.50	98.8	55	792	23	171	56	266	106
Os 5	Norway	Dyke	44.93	2.89	16.72	12.57	0.16	5.77	8.34	3.27	1.42	0.49	3.20	99.8	28	1117	23	188	36	272	33
Li11	Norway	Dyke	41.20	3.26	13.55	12.89	0.16	5.40	9.10	1.85	1.89	1.58	6.70	97.8	31	1078	32	192	45	276	6
Hov13	Norway	Dyke	45.55	3.30	14.65	12.97	0.20	4.87	6.51	3.29	2.79	1.41	3.70	99.4	56	1279	36	257	52	245	6
VK-1	Norway	Sill	43.64	2.99	15.95	11.78	0.15	4.34	6.96	3.27	1.32	0.40	7.60	98.4	31	723	26	244	33	259	11
NH13	Norway	Dyke	44.30	3.27	13.55	12.13	0.18	4.27	8.56	2.24	2.40	1.81	5.40	98.2	41	902	38	260	49	254	5
Bile 2	Norway	Dyke	41.89	3.10	16.30	12.86	0.18	4.26	7.78	2.84	1.95	0.54	7.60	99.4	64	693	37	376	67	365	32
Os 2	Norway	Dyke	49.04	2.41	15.86	9.47	0.15	4.14	5.16	4.18	3.35	0.73	4.50	99.1	89	743	29	264	53	234	20
GR12	Norway	Dyke	50.22	1.82	15.52	8.09	0.16	3.81	4.41	4.54	1.26	0.45	7.50	97.8	34	199	39	319	53	155	27
FBU-1	Norway	Dyke	52.75	2.13	15.03	9.31	0.16	3.13	4.71	3.80	2.59	0.51	5.70	100.0	65	677	35	276	46	162	6
L2	Norway	Dyke													14	1340	41	367	39	235	265
Li 13	Norway	Dyke	53.41	1.78	17.22	8.75	0.22	1.72	3.55	4.90	5.05	0.98	0.90	98.6	186	465	74	1321	258	33	6
HG 1	Norway	Dyke	51.19	1.73	18.06	8.51	0.25	1.57	3.69	4.57	4.83	0.94	3.30	98.8	112	730	69	1249	238	35	6
Hus 2	Norway	Sill	59.01	0.89	16.21	6.11	0.18	0.81	2.84	4.20	5.72	0.27	2.50	98.8	186	185	65	1291	211	17	6
SL-1	Norway	Sill	68.87	0.31	16.23	1.91	0.14	0.12	0.29	6.17	4.87	0.03	0.70	99.7	114	88	55	599	181	3	4
Vo-4	Norway	Sill	69.52	0.18	15.04	2.36	0.05	0.11	0.65	5.01	5.26	0.01	0.90	99.1	202	30	69	474	165	2	6

Estimated relative accuracy due to calibration errors ± 1%. Total Fe as Fe_2O_3. Samples arranged by location and ordered by decreasing MgO content

mafic and there is an approximately equal division between tholeiitic and alkaline types (5:7).

Tholeiitic intrusions

A total of 24 new tholeiitic samples were analysed, the majority of which are from Scotland (15), with five from Sweden and four from Norway (Table 1, Appendix 1). SiO_2 ranges from 43.6 to 52.3 wt% (Fig. 3). Clear compositional differences are evident between countries. The Norwegian samples are characterised by lower SiO_2, higher TiO_2 and CaO than the Scottish samples (Fig. 3). The Swedish samples are the most primitive with high MgO contents, albeit at intermediate SiO_2 values. They have high CaO similar to the Norwegian samples but lower TiO_2 and Fe_2O_3.

When considered as a whole, the trace element data for the tholeiitic intrusions have significant scatter when plotted against indices of fractionation such as MgO. However, there are general trends of decreasing concentrations of elements compatible in the mantle, e.g. Ni (140–15 ppm) and Cr (215–20 ppm). Clearly these samples do not represent primitive mantle melt compositions (Wood et al. 1979). In terms of the more immobile high field strength elements (HFSE; Zr, Ti, Nb, Y), all samples are enriched with respect to primitive mantle (and N-MORB) (Wood et al. 1979; Sun and McDonough 1989) with Zr: 80–268 ppm, Nb: 7.5–28 ppm, Ti: 10,730–19,184 ppm and Y: 21–42 ppm (Table 1, Appendix 1).

A selection of representative samples from each country is presented in Fig. 4. Variation in Rb and Ba is potentially a consequence of alteration. The majority of the samples show relatively smooth normalised incompatible element patterns except at Ba, Th, Ta, Nb, Sr, Zr and Ti. Examining the trace element data, country by country, highlights the variations. Of the samples analysed from Norway, the Kongsberg sample (KB 1) records the greatest enrichment accompanied by negative Nb, Sr and Ti anomalies. The Hisøy sample HY 2 has negative Th and Sr anomalies, a positive Ba anomaly, no Ti anomaly and has higher trace elemental concentrations than the other Hisøy samples.

Table 3 Additional trace element analyses by ICPMS on selected Carboniferous–Permian intrusions

Sample	Country	La	Ce	Nd	Sm	Eu	Tb	Yb	Lu	Th	U	Ta	Hf
DCW-1	Scotland	16.4	40.8	24.9	6.2	2.0	1.1	2.4	0.5	1.6	0.4	1.2	4.5
MdC-1	Scotland	16.1	40.0	24.5	6.2	2.0	1.1	2.7	0.4	1.8	0.4	1.2	4.8
LC-1	Scotland	43.0	87.9	51.7	10.9	3.4	1.6	3.6	0.5	4.2	0.8	1.5	7.2
PW-1	Scotland	21.2	50.0	27.4	6.4	2.0	1.1	2.3	0.4	2.8	0.6	1.1	3.3
LC-3	Scotland	21.1	47.7	26.8	6.1	1.9	1.0	2.3	0.3	2.8	0.7	1.0	4.3
ARN-1	Scotland	17.6	39.7	22.7	5.3	22.7	0.9	2.0	0.3	2.2	0.5	0.8	3.5
Hy-1	Norway	11.7	31.0	22.0	5.8	2.0	1.0	2.5	0.4	0.7	0.2	1.0	3.8
Hy-2	Norway	16.5	43.0	29.8	7.4	2.4	1.3	3.1	0.5	0.8	0.2	0.9	4.5
Hy-4	Norway	9.8	25.8	18.2	4.8	1.8	0.9	2.2	0.3	0.7	0.2	0.8	3.4
KB-1	Norway	24.9	56.9	31.7	7.2	2.3	1.2	3.2	0.5	3.1	0.7	1.2	6.0
ML-1	Sweden	25.6	58.7	32.6	7.5	2.4	1.3	3.3	0.5	3.2	0.7	1.2	5.9
D2	Sweden	13.1	32.5	20.5	5.2	1.7	0.9	2.2	0.3	1.4	0.4	0.9	3.9
BIL-1	Sweden	12.0	26.0	15.0	4.6	1.7	0.8	1.9	0.3	1.0	0.3	0.6	2.9
CK-1	Scotland	22.6	49.9	26.5	5.4	1.6	0.7	1.6	0.2	3.0	0.8	2.3	3.7
Hh-1	Scotland	14.3	31.8	17.7	3.9	1.3	0.6	1.6	0.2	1.7	0.5	1.4	2.7
Stc-4	Scotland	58.0	15.0	52.3	9.6	2.9	1.2	1.9	0.3	7.9	1.9	5.0	6.7
Moy5	Scotland	35.9	78.6	39.0	8.2	2.6	1.1	1.5	0.2	4.3	1.1	2.9	6.9
A7ii	Scotland	45.2	95.0	45.3	8.7	2.7	1.1	1.6	0.2	5.4	1.4	3.3	8.0
NB-1	Scotland	59.3	122.9	56.6	10.9	3.2	1.6	3.4	0.5	8.1	2.3	4.7	8.6
TK-1	Sweden	60.7	121.8	50.6	8.3	2.5	1.0	2.3	0.4	7.6	2.1	4.1	4.0
HV2	Sweden	37.3	84.5	43.9	8.4	2.6	1.2	2.7	0.4	3.3	0.9	2.3	5.6
HV1	Sweden	46.4	105.8	56.3	10.7	3.2	1.5	3.3	0.5	3.3	0.9	2.8	6.3
Al-1	Sweden	32.0	72.7	38.8	7.5	2.4	1.0	2.4	0.4	2.2	0.6	1.9	4.6
M1	Sweden	26.6	62.4	34.4	6.9	2.2	0.9	2.1	0.3	1.8	0.5	1.8	4.9
VB2	Sweden	81.6	175.5	74.5	12.8	3.3	1.7	4.3	0.6	12.4	3.9	5.9	13.5
HvS1	Sweden	81.3	175.4	74.7	12.8	3.4	1.7	4.3	0.7	12.7	3.9	5.9	13.2
JN-1	Norway	21.1	50.8	28.1	6.2	1.9	0.9	1.6	0.2	2.0	0.5	1.9	3.9
Vo-1	Norway	34.2	68.7	31.6	6.2	2.2	0.9	2.0	0.3	3.9	0.9	3.1	3.9
Os 5	Norway	31.3	71.0	37.4	7.2	2.3	0.9	1.8	0.3	2.2	0.7	2.4	4.6
Li11	Norway	47.4	108.7	60.6	11.9	4.1	1.5	2.4	0.4	2.8	0.7	2.5	4.3
Hov13	Norway	62.0	139.0	72.4	14.2	5.0	1.8	2.8	0.4	3.7	1.0	3.1	6.3
VK-1	Norway	26.5	64.1	34.9	7.3	2.4	1.0	2.0	0.3	2.5	0.8	2.1	5.4
NH13	Norway	58.9	123.0	69.9	13.3	4.3	1.7	2.8	0.4	2.9	0.8	2.8	5.6
Bile 2	Norway	67.7	151.9	70.4	13.8	4.3	1.7	3.1	0.5	8.3	2.1	4.2	9.7
Os 2	Norway	55.0	116	54	9.6	2.9	1.2	2.3	0.4	6.7	2.1	3.2	6.4
GR12	Norway	47.1	96.9	51.4	10.0	2.7	1.5	3.3	0.5	6.5	2.0	2.8	7.8
FBU-1	Norway	43.1	95.4	45.2	9.2	2.9	1.3	3.2	0.5	5.8	1.6	3.2	7.2
L2	Norway	91.6	177.4	76.5	13.8	4.2	1.7	2.7	0.4	14.5	3.2	7.0	7.7
Li 13	Norway	156.5	303.9	128.8	22.2	5.1	3.0	6.3	0.9	28.1	7.8	14.2	22.8
HG 1	Norway	136.0	292.7	117.5	22.5	5.6	2.9	6.2	0.9	25.9	6.9	14.1	23.1
Hus 2	Norway	134.8	253.3	103.3	17.1	3.7	2.5	6.0	0.9	30.8	8.6	9.7	24.4
SL-1	Norway	150.8	290.1	116.6	17.8	3.4	2.2	5.0	0.8	23.4	5.3	10.5	13.9
Vo-4	Norway	157.0	288.5	111.0	18.0	0.6	2.4	6.4	1.0	32.5	7.6	8.8	12.9
JB-3	Standard	8.3	21.6	16.1	4.3	1.3	0.8	2.5	0.4	1.3	0.5	0.1	2.9
JB-3	Standard	8.0	20.9	15.6	4.2	1.3	0.8	2.5	0.4	1.3	0.5	0.2	2.9
JB-3	Standard	8.2	21.3	15.9	4.3	1.3	0.8	2.5	0.4	1.3	0.5	0.1	2.9

Standard used JB3 (Govindaraju 1994). Calibrated using W2 (USGS); MAR (MORB) and K1919 (Kilauea)

HY 1 and HY 4 are similar with the exception of a large positive Ba anomaly (HY 1). In terms of the most incompatible trace elements, the Hisøy samples are some of the most primitive samples analysed in this study with relatively low concentrations of large ion lithophile (Rb, Ba) and high field strength elements (Th, Nb, Zr) (Fig. 4a). Swedish sample ML 1 and the Norwegian sample KB 1 have indistinguishable compositions. The other Swedish sample D2 has a flat profile broadly similar to E-MORB (Fig. 4b).

Scottish samples have the greatest trace element variation. Normalised trace element patterns vary from smooth to those characterised by both positive and negative Nb, Sr, Zr or Ti anomalies (Fig. 4c). The samples can be divided into three groups with DCW-1 and MdC-1 (Group 1) having negative Sr anomalies and positive Nb–Ta and Ti anomalies. LC-1 has a similar profile to ML1 (Sweden) and KB-1 (Norway), with the exception of lower Ba (Fig. 4). LC-1 is more enriched than Group 1 and has pronounced negative

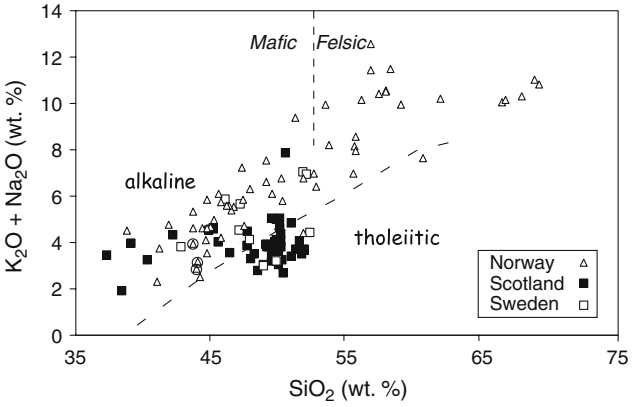

Fig. 2 Total alkali versus silica diagrams used to classify the different rock types (after Le Maitre et al. 1989). Note the number of samples quoted in the text may differ slightly from the number seen in the figure as not all samples were analysed for all elements. Samples from Norway with circle background are those reclassified on the basis of their Nb/Y and Zr/Nb trace element ratios

Nb–Ta, Sr and Ti anomalies (Group 2). The remaining samples display minor negative Nb–Ta anomalies and no Sr or Ti anomalies (Group 3). The fractionation of heavy REE is remarkably similar for all samples. There is considerable compositional variation between the different tholeiitic dykes and sills from each of the countries (Fig. 4) indicating varying melt source and petrogenetic evolution.

Investigating the co-variation of incompatible elements including Y, Ti, Th, Nb, Zr and La provides first order evidence that variations in melting, fractionation, assimilation and source composition is recorded in these sample sets (Figs. 3, 5). Overall Y/La decreases markedly with increasing La, suggesting that variable degrees of melting might be important (Peate 1997). The spread of the Scottish data, however, is greater than elsewhere and implies that variable trace element enrichment in the mantle source may be locally important (Fig. 5). The samples from Sweden tend towards lower La, Zr, Ti and Th than the samples from Scotland with the exception of sample ML-1 from Molle, which has a similar geochemical signature to KB-1 from Norway (Figs. 3, 5). The Norwegian samples trend towards high Y/La and Ti and low Th when compared with both Scotland and Sweden.

Fractional crystallization—tholeiites

Tholeiitic intrusions have low magnesium numbers (mg # < 52) and Ni contents <107 ppm (Table 1).

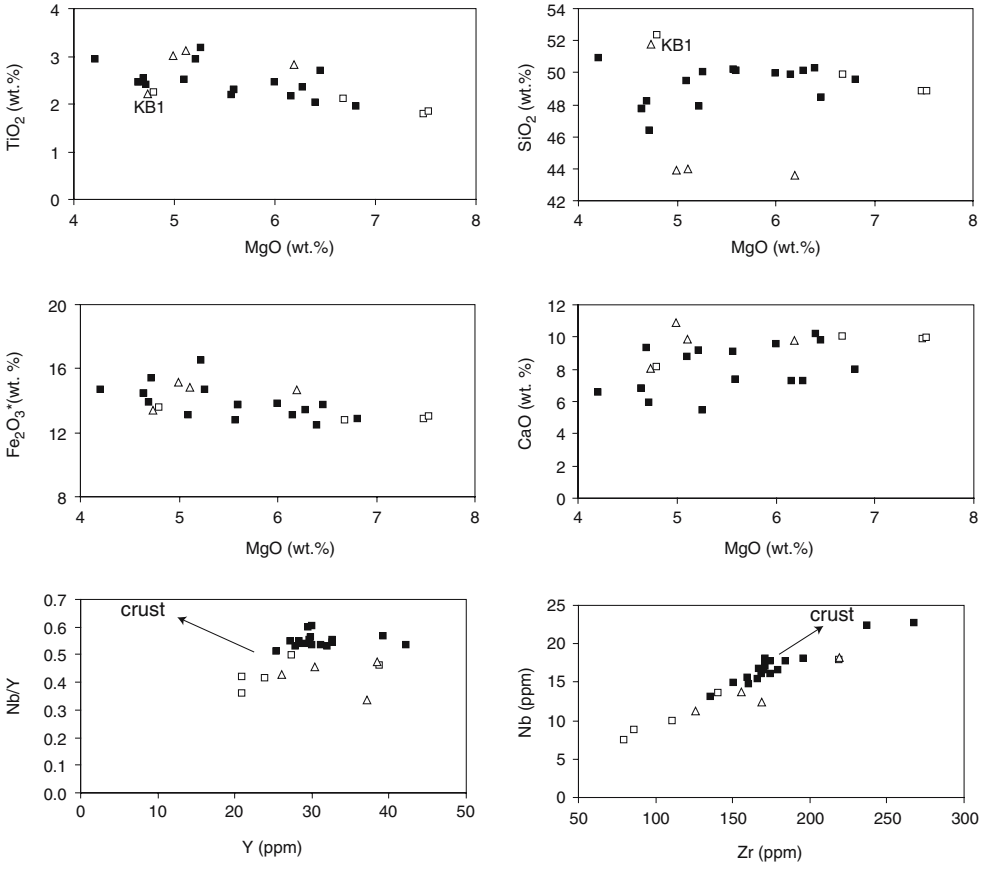

Fig. 3 Major and trace element variation diagrams for the tholeiitic samples highlighting the regional variations. *Crust* represents average upper crust (Taylor and McLennan 1985). Norway *open triangles*; Sweden *open squares*; Scotland *filled squares*

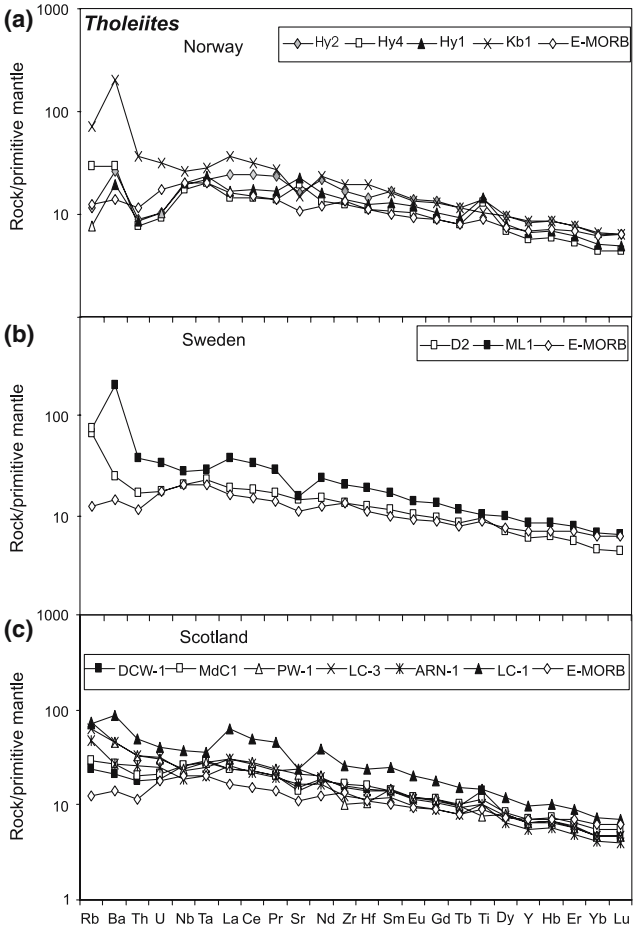

Fig. 4 Primitive mantle normalised diagram of Carboniferous–Permian tholeiites from **a** Norway, **b** Sweden and **c** Scotland. Normalising values and E-MORB composition after Sun and McDonough (1989)

Application of the Petrolog 2.1 program (http://www.geol.utas.edu.au/~leonid/) to the major element analyses of the most primitive samples from each of the countries indicates that low pressure (0.1 GPa) fractionation of a pyroxene + plagioclase + olivine mineral assemblage had an important control on the magmatic evolution in all countries (Fig. 3). These assemblages are consistent with the observed phenocryst petrography, and Sr and Ti anomalies are consistent with accumulation/removal of plagioclase, Ti-rich pyroxene, Ti-amphibole or Ti-rich oxides. In general TiO_2 and Fe_2O_3 are low compared to most continental tholeiites (e.g. Peate 1997) suggesting that either the source was depleted in these elements or that the oxides saturated early.

On process identification diagrams such as Th/Nb versus Th (Fig. 5b) crystal fractionation produces horizontal vectors with constant Th/Nb. The gradient in Fig. 5b indicates that, although fractional crystallisation is an important process, the effects of contamination and/or source variation(s) are also apparent. For example, Th/Nb ratios vary from 0.08 to 0.2 in the Scottish tholeiite samples. Th/Nb ratios are distinct between groups recognised earlier on the basis of pronounced positive and negative Nb–Ta, Ti and/or Sr anomalies. Group 1 have the lowest Th/Nb. Group 2 has high Th, La and Th/Nb values, while Group 3 is intermediate between Groups 1 and 2. The Norwegian samples have remarkably low Th/Nb and Th/Ta similar to N-MORB (0.05, 0.6, respectively; Sun and McDonough 1989). The Swedish samples plot at higher Th/Nb and marginally higher Th than the Norwegian samples. ML1 and KB1 are again notable exceptions (Fig. 5b).

Modelling of the assimilation and fractional crystallisation (AFC) process was performed using equation 4.22 of Rollinson (1993). The primitive sample (HY4) from Norway was chosen as the starting composition because of its high MgO and Ni contents and low Nb and Th. The fractionating assemblage used consisted of clinopyroxene (50%), plagioclase (40%), olivine (5%) and magnetite (5%) and r, the rate of crustal assimilation relative to fractional crystallisation, was kept constant at a value of 0.25. As discussed previously the majority of the Norwegian rocks appear uncontaminated; however, sample KB-1 can be modelled by ~12% AFC if the contaminant is similar to a Sveconorwegian granite (Nb: 38 ppm, Th: 51 ppm, Andersen and Knudsen 2000). The entire spread in the Scottish data can be modelled by <20% AFC from a similar starting point and using the same r value and contaminant. The Swedish samples require a more enriched mantle source as a starting composition, apart from ML-1, which is similar to the KB-1 intrusion from Norway.

Melting and source variations—tholeiites

Isotope studies have demonstrated that the mantle is exceedingly heterogeneous being continuously enriched during subduction processes and by metasomatism, and depleted during melt extraction (Zindler and Hart 1986). Traditionally sources have been described in terms of a tetrahedron which features depleted mantle (DMM) and different varieties of enriched mantle, EMI (metasomatised lithosphere), EMII (subducted continental material) and HIMU (oceanic lithosphere) (Zindler and Hart 1986). The chemistry of the Carboniferous–Permian dykes and sills has been compared with a collection of OIB-like basalts (EMI, EMII, HIMU) (E-A. Dunworth, personal communi-

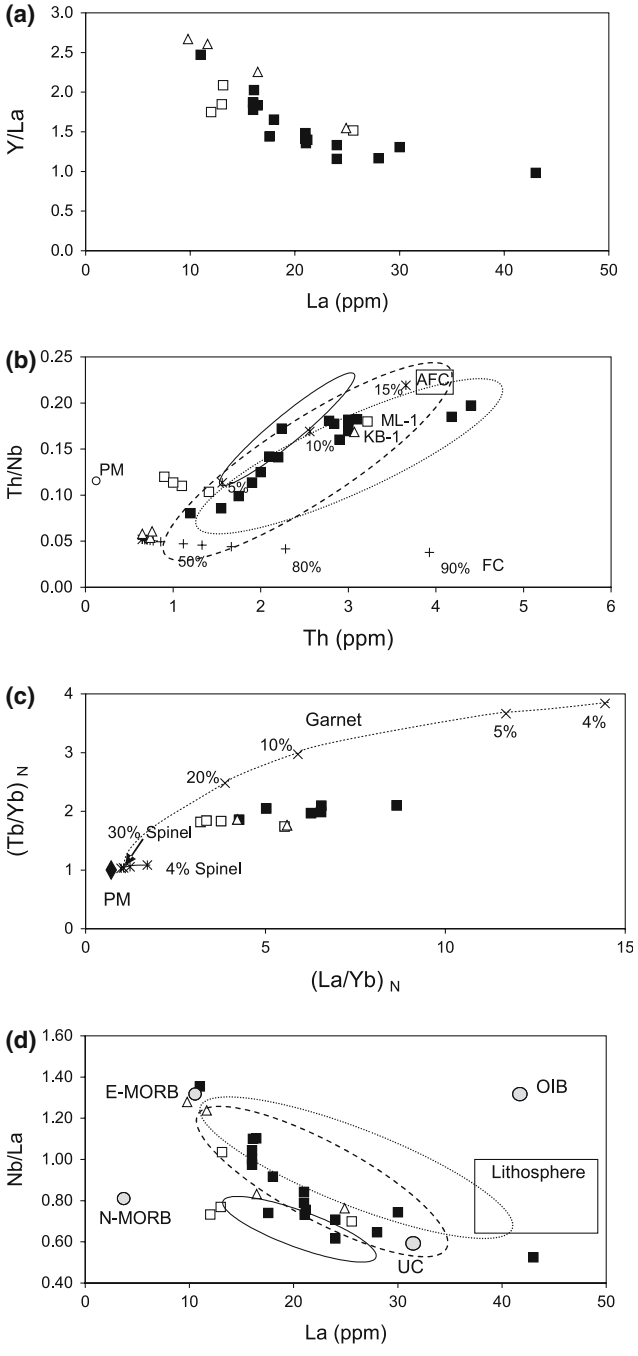

Fig. 5 Element–element, ratio–element and ratio–ratio diagrams of Carboniferous–Permian tholeiitic samples from Northern Europe. Symbols as in Fig. 2. **a** Y/La versus La (ppm); **b** Th/Nb versus Th (ppm) *FC* fractional crystallisation modelled trend, *AFC* modelled assimilation and fractional crystallisation using Hy 4 as the starting composition. Contaminant Th: 25 ppm, Nb: 17 ppm is within the range for normal Sveconorwegian granites (Andersen and Knudsen 2000). Percentages are indicated at appropriate intervals. Fields for tholeiitic lavas and intrusions from Norway solid field (Neumann et al. 1988); Sweden dotted field (Obst et al. 2004) and Scotland dashed field (MacDonald et al. 1981; Smedley 1988), **c** $(Tb/Yb)_N$ versus $(La/Yb)_N$. Non-modal batch melting curves generated from a primitive mantle starting composition (Sun and McDonough 1989). Percentage melting indicated by *crosses*, see text for details. **d** Nb/La versus La (ppm). *Open rectangle* represents West Greenland lithospheric component after Larsen et al. (2003). Norway *open triangles*; Sweden *open squares*; Scotland *filled squares*

cation) and previously published data on lavas from Norway (Neumann et al. 1988, 2004) and Scotland (Smedley 1988; Wallis 1989), and with intrusions from Sweden (Obst et al. 2004), Scotland (MacDonald et al. 1981) and Norway (Neumann et al. 2004). All samples show a depletion of heavy REE relative to middle REE with $(Tb/Yb)_N$ (subscript N denotes chondrite normalised) ratios ranging from 1.75 to 2.10 (Fig. 5c). Such depletions are characteristic of the involvement of residual garnet during the evolution of the magma or in its source (Peate 1997). The majority of the Scottish samples trend towards higher $(Tb/Yb)_N$ and $(La/Yb)_N$ (>1.95 and >5, respectively) than the Norwegian and Swedish samples ($(Tb/Yb)_N < 1.85$; $(La/Yb)_N < 5.8$) (Fig. 5c).

To constrain the depth(s) of melting, samples were modelled using non-modal batch partial melting equations. In order to minimise the influence of fractionation and crustal contamination, only samples with >5 wt% MgO have been modelled. The curves plotted in Fig. 5c are for melting of garnet lherzolite and spinel lherzolite. These curves were calculated using modal compositions and phase proportions entering the melt of ol:opx:cpx:sp = 20:20:55:5 and ol:opx:cpx:gnt = 20:20:30:30 for spinel and garnet lherzolite respectively (Ellam 1992). A primitive mantle source was used to define the starting composition (Sun and McDonough 1989). All samples are displaced to the right of the melting curve for garnet lherzolite indicating an enriched source region. The Scottish samples were generated by a smaller degree of melting (<15%) than those from Norway and Sweden (<20%). Such variation in the degree of melting between countries and within Scottish samples is consistent with the observed trace element variation discussed previously and cannot be ascribed solely to an AFC process.

The large inferred degrees of melting combined with variable Ti anomalies and high La/Ta and Th/Nb ratios indicate potential source variations with mixing of at least two melt sources as well as an upper crustal component (Peate 1997; Kirstein et al. 2000).

The variation of Nb/La with La (Fig. 5d) also indicates the involvement of at least two end member sources, the first with high Nb/La and low La and the second with high La, low Nb/La. The Scottish and Swedish samples have higher La/Sm and La/Ta ratios

and lower Nb/La than the uncontaminated Norwegian samples, which are similar to enriched-MORB (Fig. 6). Despite the close geochemical affinity of certain samples to E-MORB and the potential to explain some of the data by variation in the degree of melting, the entire data set is best explained by three-component mixing. We interpret one component as similar to E-MORB derived as melts from an enriched asthenospheric component. The variation in La/Sm and La/Ta requires addition of a lithospheric mantle component and locally the involvement of upper continental crust. Similar conclusions have been drawn from previous efforts to model the dolerite intrusions of Scania (Obst et al. 2004) and the Norwegian tholeiites (Neumann et al. 2004).

Alkaline mafic and felsic intrusions

The alkaline intrusive rocks represent the majority of the samples (67%) and span a broad range in chemical composition from ultrabasic (37 wt% SiO_2) to intermediate and felsic (51–70 wt% SiO_2). After a preliminary investigation of major and trace elements these samples have been subdivided into mafic (<55 wt% SiO_2) and felsic groups (Fig. 2). However, the effects of open system processes on the petrogenesis are discussed together. The majority of the samples that define the large range in SiO_2 are from Norway (59). All samples from Sweden (7) and Scotland (9) are mafic to intermediate in composition (37–53 wt% SiO_2).

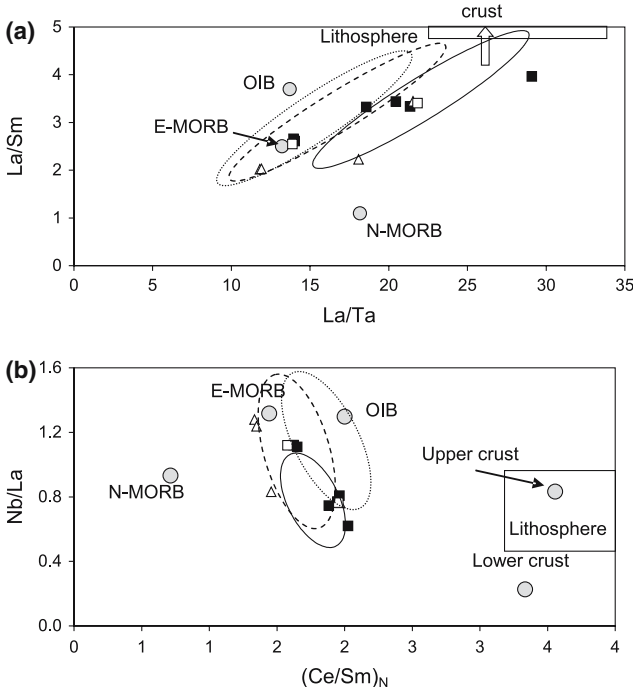

Fig. 6 **a** Nb/La versus $(Ce/Sm)_N$ and **b** La/Sm versus La/Ta of Northern European Carboniferous–Permian tholeiitic intrusions. Average OIB, E-MORB, N-MORB data from Niu and O'Hara (2003). Crust from Taylor and McLennan (1985). Tholeiites from Norway solid field (Neumann et al. 1988); Sweden dotted field (Obst et al. 2004) and Scotland dashed field (MacDonald et al. 1981). *Open rectangle* represents Greenland lithospheric component (Larsen et al. 2003)

The major element data define general inter-element trends, with CaO, Fe_2O_3, TiO_2, MgO decreasing and Na_2O, K_2O increasing with increasing SiO_2 (Fig. 7). Incompatible trace elements such as Nb and Zr are particularly enriched in some of the evolved felsic samples, especially the rhomb porphyries, possibly due to the presence of halogen-rich volatiles in the melt during crystallisation (Kirstein et al. 2001) (Fig. 7).

Focussing initially on the mafic samples, regional compositional differences can be identified on major element diagrams (Fig. 7). The samples from Scotland, unlike the majority of samples from Norway and Sweden, tend towards higher MgO and Zr and lower Fe_2O_3 and K_2O abundances at moderate SiO_2, with one notable exception, sample NB-1, which is the most evolved Scottish sample (Table 1). The majority of samples from Sweden and Norway have <6 wt% MgO (Fig. 7). A notable exception is sample TK-1 from Sweden (MgO (wt%) = 10.25), which unlike the other Swedish samples contains olivine in thin-section. Samples Bile1, Bile3, Vo-1 and JN-1 from Norway also have high MgO (7–12 wt%) and contain significant olivine ± amphibole ± biotite (up to 30%).

Majority of samples from Sweden are more evolved (lower MgO) than Scottish samples and have higher TiO_2, Fe_2O_3 and Na_2O and lower CaO consistent with having undergone greater fractional crystallisation. Some of the Norwegian samples overlap the Swedish group in composition. However, seven samples are more evolved and have lower MgO, TiO_2, Fe_2O_3 and CaO and higher SiO_2 and Na_2O than the rest of the Norwegian alkaline samples (Fig. 7). These latter Norwegian samples have comparable appearance and composition to a group of intrusives termed maenaites (Scott and Middleton 1983; Sundvoll et al. 1990). The term refers to feldspar-rich intrusions which have low SiO_2 (44–51 wt%) and high alkali and incompatible element concentrations (e.g. Nb 53–107 ppm, Zr 276–470 ppm) (Scott and Middleton 1983). These samples are identified on all relevant figures with a separate symbol to distinguish them from the other Norwegian mafic samples.

The incompatible element abundances of the more basic samples (SiO_2 < 50 wt%) have been normalised

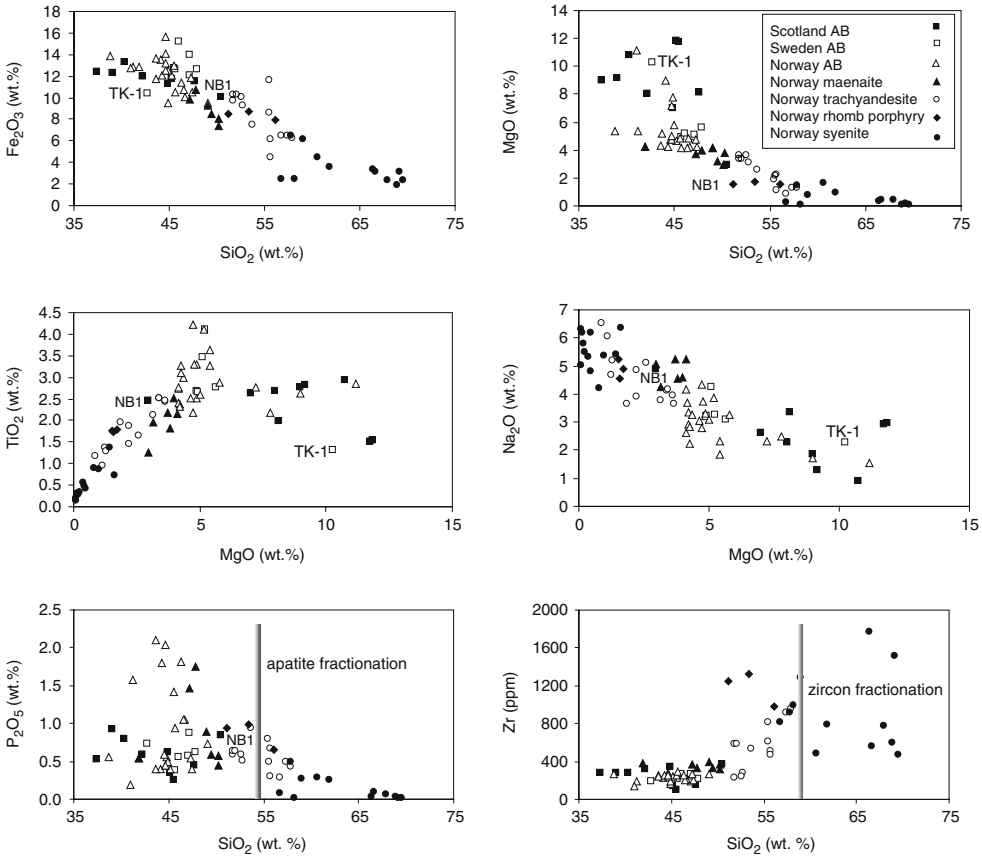

Fig. 7 Major and trace element variation diagrams for Carboniferous–Permian alkaline intrusions from northern Europe

to primitive mantle and compared with OIB (Figs. 8, 9a). Samples from each country show a wide variation of trace element behaviour particularly in terms of the presence or absence of Ba, Sr and Ti anomalies, while all regions show negative Hf–Zr anomalies, most pronounced in Norway (Fig. 8). Such Sr and Ti anomalies may be a source feature or the result of preferential removal of plagioclase and magnetite from the melt. Compared to OIB the maenaite samples are enriched in all elements from Th to Lu, except for pronounced negative Sr and Ti anomalies consistent with feldspar and magnetite fractionation (Fig. 9a).

Overall, mafic samples from Scotland show the largest range in incompatible element enrichment, bracketing the samples from Sweden and Norway. When compared with the Carboniferous–Permian tholeiite data the alkaline intrusions tend towards higher Zr/Y (<6.3 to >5.2), $(Ce/Sm)_N$ (<1.9 to >2.1), $(La/Yb)_N$ (<6.5 to >9) and $(Dy/Yb)_N$ (<1.6 to >1.5, respectively). Metasomatic enrichment of the upper mantle prior to melting can produce melts enriched in Ba, Sr, Nb and P. Mantle and crustal xenoliths brought to the surface in Scotland during the Carboniferous–Permian do in fact show evidence of widespread metasomatism by Fe, Ti, HFSE, LILE and volatile-rich melts (Upton et al. 2004).

Felsic alkaline intrusions

The earliest Carboniferous–Permian intrusions sampled are microsyenites and syenites. These samples are highly evolved and vary from 56 to 70 wt% SiO_2 (Fig. 7). The RP and trachyandesites are intermediate in composition, with SiO_2 ranging from 51 to 56 wt% and 52 to 57 wt%, respectively (Fig. 7). Where the groups overlap in terms of SiO_2 content the RP tend towards higher TiO_2, Fe_2O_3, CaO, MnO and lower Na_2O, K_2O than the microsyenites (Fig. 7, Table 1). The RP group overlaps the trachyandesites in TiO_2 and Fe_2O_3, although the trachyandesites plot at higher CaO and lower Al_2O_3, K_2O and MnO (Fig. 7, Table 1). The trachyandesites clearly record evidence of apatite fractionation commencing at a SiO_2 value of ~54 wt%, while the decrease of Zr in some of the syenites indicates zircon fractionation at a SiO_2 value of ~58 wt%. The involvement of apatite during fractional crystallisation is recorded by relatively low Sm in the syenites and trachyandesites. The RP group is in general more trace element enriched than the trachyandesites and syenites at similar SiO_2 values.

A number of similarities in major and trace element composition can be recognised between the rhomb porphyry and maenaite groups (Fig. 7). In particular,

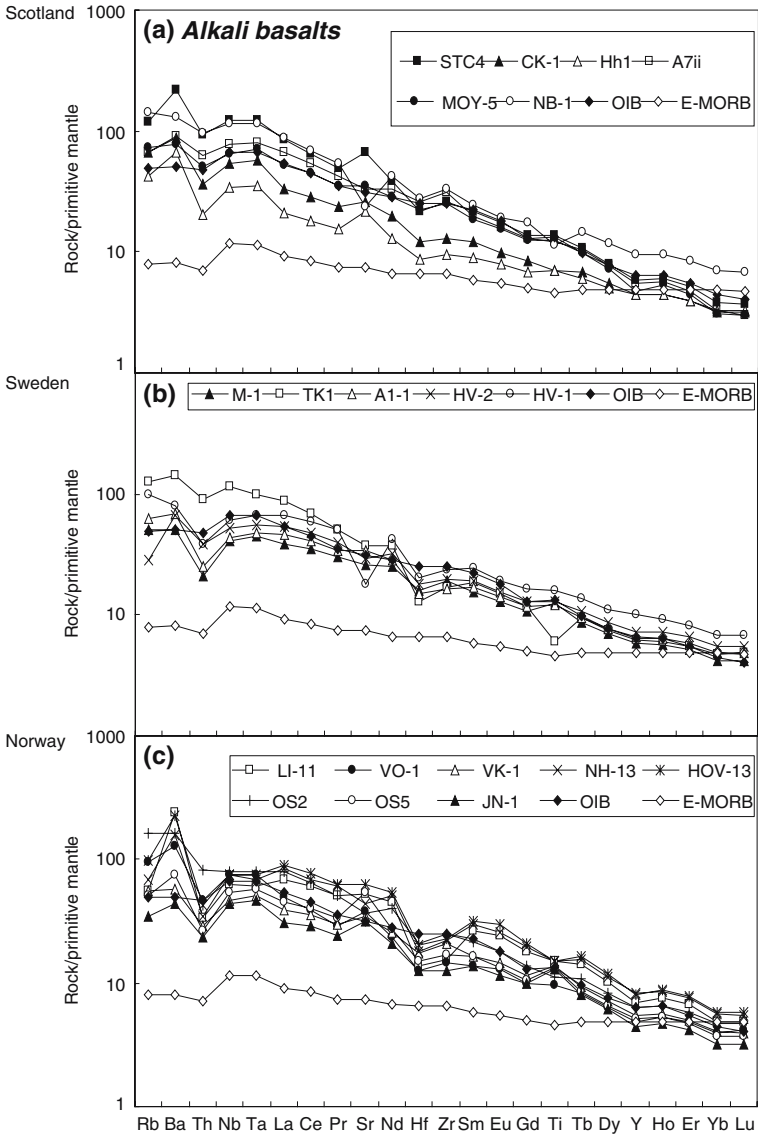

Fig. 8 Primitive mantle normalised incompatible element diagrams for Carboniferous–Permian alkaline samples from **a** Scotland, **b** Sweden and **c** Norway. Data source as in Fig. 4

the groups share the same range in Fe_2O_3, TiO_2, Na_2O and P_2O_5. The rhomb porphyries are, however, more evolved and contain higher SiO_2, Zr, Nb and lower amounts of CaO and MgO (Fig. 7, Table 1). Primitive mantle normalised incompatible element plots highlight remarkably similar compositions for these two groups with large negative Ba, Sr and Ti anomalies that clearly reflect feldspar and magnetite fractionation. The maenaites are less trace element enriched, which suggests that either they are larger degree melts or they originate from a less enriched source (Fig. 9a).

When all the evolved felsic samples are normalised to an alkali basalt (Vo-1, Table 2) a number of striking features can be appreciated (Fig. 9b). First, all samples from the three groups have marked negative Ba, Sr, and Ti anomalies, with minor Eu anomalies also indicating the importance of feldspar and magnetite fractionation. Second, the behaviour of Zr is highly variable with the syenites indicating Zr depletion consistent with zircon fractionation, while the trachyandesites and RP indicate overall trace element enrichment.

Fractional crystallization—alkaline

All the samples analysed have a mg # < 67 clearly indicating that they are not primitive mantle melts, although some of the samples are less evolved than the tholeiites discussed previously. From major and trace element variation diagrams it is evident that fractionation ± assimilation has played an important role in the petrogenesis of these samples, particularly those from Sweden and Norway that show decreasing TiO_2, Fe_2O_3 and CaO with decreasing MgO (Fig. 7). The maenaites

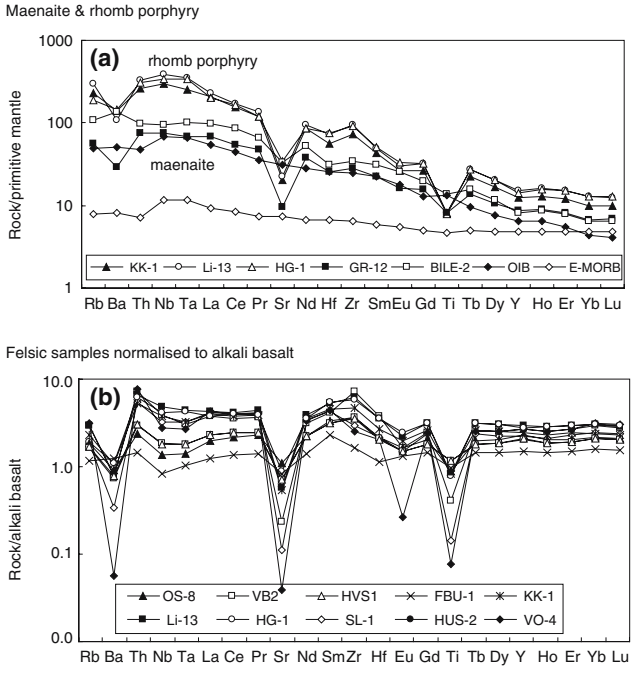

Fig. 9 **a** Primitive mantle normalised incompatible element diagrams for maenaite and rhomb porphyry samples. Average OIB and E-MORB compositions from Sun and McDonough (1989). **b** Alkali basalt normalised incompatible element diagrams for felsic samples. Normalised to Vo-1 from Norway, Table 2

plot on a continuum of the alkali basalt trend at lower MgO, TiO_2, Fe_2O_3 and CaO and higher Na_2O (Fig. 7). Norwegian and Swedish samples plotting off this general trend contain olivine and amphibole (visible in thin section), which increases their MgO content. In general, the Scottish samples are less evolved with the highest average MgO contents. The trend of Scottish samples is displaced from the main trend defined by the Swedish and Norwegian samples, but the overall trend of decreasing Fe_2O_3 and increasing Na_2O with decreasing MgO is maintained and is consistent with high level fractional crystallisation.

Fractional crystallisation is unlikely to have occurred in isolation and there is considerable evidence, including variable Th/Nb ratios, to suggest that crustal assimilation occurred. The effects of fractional crystallisation and assimilation have been modelled and are illustrated on a diagram of Th/Nb versus Th (Fig. 10a). If the most primitive Norwegian sample JN-1 is used as a starting composition, much of the range in alkali basalt composition in Norway can be modelled by <15% AFC if r = 0.2 and a Sveconorwegian granite composition is used as the assimilant (Andersen and Knudsen 2000) (Fig. 10a). Os 2 appears to be the most contaminated alkali basalt with 35% AFC required to explain its high Th/Nb using a constant r value of 0.2.

The maenaite samples plot in two regions of the diagram with some overlapping with the relatively uncontaminated alkali basalts but, the majority plot at high Th/Nb. Os 2 plots in the same region of the diagram as these high Th/Nb maenaite samples, which suggests that the maenaites are either highly contaminated alkali basalts or they have been derived from a separate source characterised by high Th/Nb. Such a large amount of contamination is not consistent with the major element data, as Os 2 contains, for example, just 49 wt% SiO_2. We therefore conclude that there is

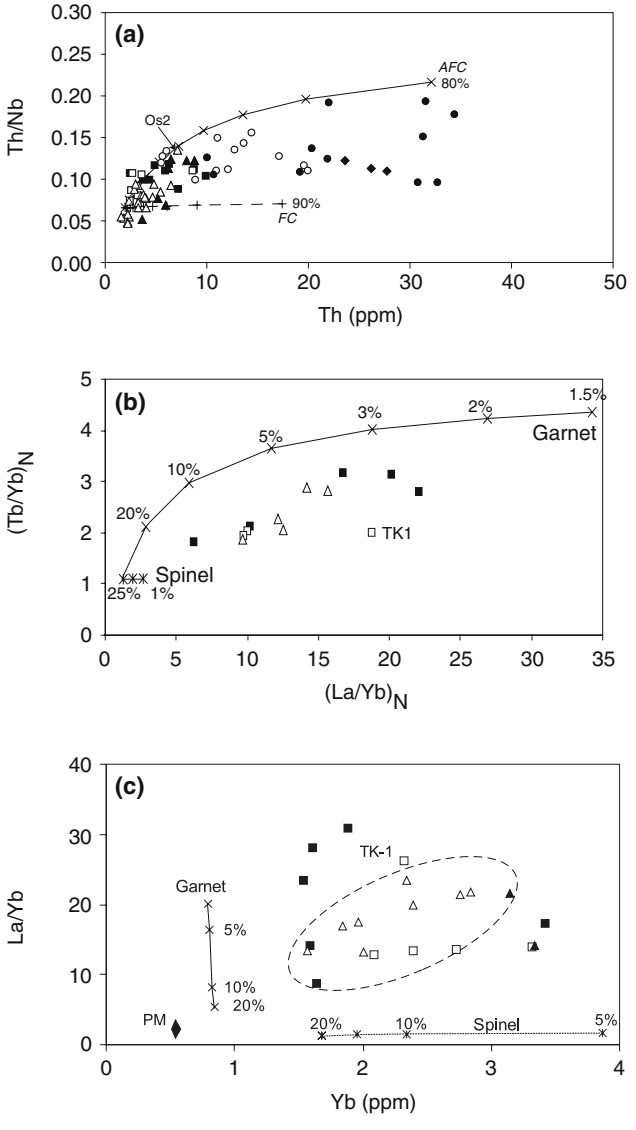

Fig. 10 Trace element ratio–element composition diagrams for Carboniferous–Permian alkaline intrusions from northern Europe. Symbols as in Fig. 7. **a** Th/Nb versus Th ppm includes fractional crystallisation (*FC*) and assimilation and fractional crystallisation (*AFC*) models defined in Fig. 5 with a starting composition JN1 from Norway. **b** $(Tb/Yb)_N$ versus $(La/Yb)_N$ and **c** $(La/Yb)_N$ versus Yb ppm include melting models as described in Fig. 5

significant source heterogeneity among the alkaline magmas even in a single magmatic suite. Similarly, the large variation in some trace elements in the trachyandesite group (e.g. Th) requires a minimum of 60% fractional crystallisation even assuming that Th is totally incompatible throughout the crystallisation history. The microsyenites and RP groups are similarly difficult to relate to the alkali basalts or maenaites, as extreme AFC of between 85 and 95% at $r = 0.2$ is required from a starting composition similar to sample JN1. Such high AFC values are completely unrealistic for the petrogenesis of the trachyandesites, rhomb porphyries and syenites. Consequently the effects of source heterogeneity and the degree of melting are further investigated below.

The Swedish samples can be modelled by <30% AFC using an r value of 0.2 from a source similar to M1, with the usual exception of TK-1 that contains higher Th at similar Th/Nb. The variation in the Scottish samples requires up to 65% AFC of a low Th (10 ppm), Nb (8 ppm) at $r = 0.2$ (Fig. 10a). These values are also unrealistic in terms of heat budgets and an alternative model of mixing different sources with variable Th/Nb is preferred. Source heterogeneity along with variations in the degree of melting thus appears to be a characteristic of the Carboniferous–Permian magmas generated in Norway, Sweden and Scotland.

Melting and source variations—alkaline

In order to minimise the effects of fractionation and crustal contamination, samples with >5 wt% MgO have been modelled using non-modal batch partial melting equations to constrain the depth range of melting. Figure 10b is a diagram of $(La/Yb)_N$ versus $(Tb/Yb)_N$ with curves plotted for melting of garnet lherzolite and spinel lherzolite. The melting model is that of Ellam (1992) as described above. The alkali basalt data plot below the curve that is defined by melting solely in the garnet lherzolite stability field. The displacement of the data to higher $(La/Yb)_N$ than the melting curves in Fig. 10b is greater than can be explained solely by a proportion of the melting occurring in the spinel lherzolite stability field and therefore implies that the source of the alkali basalts is more enriched than primitive mantle. Sample TK1 (Sweden) is more enriched than all other samples of similar SiO_2 (wt%) and so is not included in the following discussion. The remaining data plot along a trend sub-parallel to the melting curve of garnet lherzolite. These data could represent variable melting of an enriched source region with the smallest and largest degree melts in Scotland. In which case, the Swedish and Norwegian samples are produced by between 4 and 10% melting (Fig. 10b). A compositional gap at $(Tb/Yb)_N$ between 2.3 and 2.9 and $(La/Yb)_N$ between 12.5 and 14.2 could alternatively indicate heterogeneous sources (Fig. 10b).

La/Yb, however, is sensitive to both the degree of melting and the amount of residual garnet, whereas Tb/Yb is controlled by the amount of residual garnet (Peate 1997). Thus variations in Tb/Yb can be used to estimate the amount of residual garnet during the entire melting process and so constrain the depth of melting. Greater residual garnet increases the fractionation in Tb/Yb. Melting in the spinel stability field leads to a more gradual increase in La/Yb with little change of Tb/Yb. This reasoning suggests that the source of the most enriched Scottish samples melted entirely in the garnet stability field (high La/Yb, Dy/Yb and low Yb, Fig. 10c). In contrast, Scottish samples with lower trace element enrichment have lower La/Yb and Dy/Yb at comparable Yb implying the involvement of significant residual spinel at some stage during the melting process. La/Yb increases with increasing Yb for samples from Norway, which implies that the amount of residual garnet present is <5% but again requires that a large proportion of the partial melting occurred in the spinel stability zone (Fig. 10c). Most Swedish samples have constant La/Yb but variable Yb. The elevated La/Yb is consistent with a proportion of melting in the presence of residual garnet but the constant La/Yb with variable Yb indicates that the bulk of the melting occurred in the spinel stability field (Fig. 10c).

Source components—alkaline

Some mafic, alkaline samples from Scotland, Norway and Sweden show remarkable similarities to average OIB (Fig. 8). The minor deviations such as positive or negative Sr and Ti anomalies possibly reflect feldspar fractionation ± source enrichment. In Scotland the mantle xenolith-bearing dykes (A7ii, Moy5 and StC4) are similar to average OIB but are slightly more enriched in HFSE and LREE, and more depleted in HREE (Fig. 8). It is difficult to distinguish unambiguously between crustal interaction and the involvement of melt produced in the lithosphere on the basis of trace element abundances alone, as melt characteristics such as Ta depletion can be attributed to either crust or lithosphere (Wooden et al. 1993). Coupled variations in, e.g. La/Ta and La/Sm, can be used to assess the involvement of the crust since it is enriched in LREE. Using this rationale it is apparent that some of the

alkaline intrusions from Norway, Sweden and Scotland have an enriched, possibly lithospheric signature and can be modelled by mixing melts produced in the asthenosphere (low La/Ta) with melt from the lithosphere (high La/Ta). The alkali basalt melts from Norway with negative Ti anomalies, low Nb/La and variable Sr anomalies also plot at high La/Ta indicating mixing with a lithospheric melt source. The Swedish alkaline samples have La/Ta (14.5–16.7) and La/Sm (3.8–4.4) intermediate between the two Norwegian groups, again with the exception of TK-1, which has much higher La/Sm (Fig. 11). These samples represent small degree melts from the asthenosphere that have interacted with a small amount of lithospheric melt en route to the surface. The source of TK-1 and similar samples has clearly undergone marked enrichment ± crustal contamination.

Diagrams of La/Sm versus La/Ta and Nb/La versus $(Ce/Sm)_N$ can be used to distinguish between different types of enriched OIB-like mantle, in particular HIMU, EMI and EMII, and crustal contamination trends (Fig. 11). All Scottish samples plot in the HIMU field of the diagrams, although Hh-1 and CK-1 have lower La/Sm, La/Ta, and higher Nb/La and $(Ce/Sm)_N$ than the mantle xenolith-bearing samples. This suggests that they are possibly larger degree melts of the same dominantly asthenospheric source region, and that the source region was trace element enriched due to metasomatic processes (Figs. 8, 11). However, the relatively low La/Ta and Th/Nb ratios are inconsistent with significant crustal contamination.

Swedish samples M-1, Al-1 and HV-2 are also broadly similar to average OIB (Sun and McDonough 1989) but there are a number of differences in terms of the HFSE as the Swedish samples are depleted in Nb, Hf, Zr and Ti. TK-1 is again distinct from the majority of samples with higher La/Sm (Fig. 11), Nb/La and $(Ce/Sm)_N$. The apparent enrichment in incompatible elements and large negative Ti anomaly of TK-1 suggest an origin from a highly enriched source region. The remaining Swedish samples fall in the EMI field, consistent with the mantle in this region being enriched through previous subduction episodes. Such an enriched source region diminishes the requirement of >30% AFC modelled above. However, the more evolved rocks plot towards upper crustal compositions (Fig. 11), which suggest that some AFC has occurred.

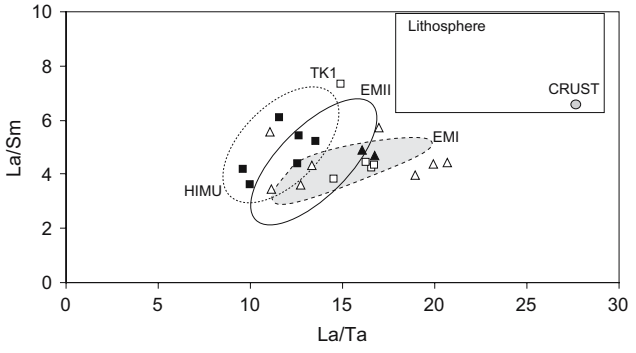

Fig. 11 La/Sm versus La/Ta diagram for Carboniferous–Permian alkaline intrusions from northern Europe. Symbols as in Fig. 7. *Grey field* represents EMI, *solid field outline* for EMII and *dashed field* for HIMU mantle components. Crust composition from Taylor and McLennan (1985). Greenland lithospheric component after Larsen et al. (2003)

The observed geochemical diversity of the alkali basalt samples from Norway requires a number of sources to explain their petrogenesis. The samples can be divided into three groups. Group 1 has negative Ti and Sr anomalies and is highly trace element enriched despite having a SiO_2 range from 41 to 45 wt%. This includes samples Li 11, NH13 and Hov13. Group 2 has positive Ti and Sr anomalies and lower incompatible element concentrations at a similar SiO_2 as Group 1, this includes JN-1, Vo-1, VK1 and Os5. Group 3 consists of the 'maenaites' (e.g. GR12 and Bile 2), which have very large negative Ti ad Sr anomalies but are not as trace element enriched as Group 1. It is evident from Fig. 11 that three distinct source regions representing mantle enriched through either subduction or metasomatism—EMII, HIMU and EMI—could be important end members in the chemistry of these samples. The relatively low Nb/La ratios, and hence high La/Ta ratios, of Group 1 suggest clear involvement of lithospheric mantle in their petrogenesis. However, they have low Th/Nb indicating possible dilution of the lithospheric enrichment by contamination with the lower crust. Group 2 samples plot in the HIMU domain; only Os 2 appears to have suffered major crustal contamination or source enrichment (modelled above). Finally, the maenaite samples from Group 3 are intermediate between the evolved samples of Group 1 and the primitive samples of Group 2 and have a marked lithospheric component (Fig. 11).

Recently, Neumann et al. (2004) compiled a summary of all Sr–Nd isotope data available for the Carboniferous–Permian magmatism of Scandinavia and northern Germany. A large variation in the range of Sr–Nd data is observed ranging from prevalent mantle (PREMA) to HIMU with crustal contamination particularly important in the petrogenesis of some basalts, the RP suite and the more evolved felsic samples. Such source heterogeneities and complex petrogenetic evolution is also characteristic of the Carboniferous–Permian magmatic products in Sweden (Obst et al. 2004) and Scotland (Upton et al. 2004). In all these regions mixing litho-

spheric and asthenospheric melts with variable amounts of crustal assimilation is required to explain observed major-, trace-element and isotope variations.

Discussion

The diversity of magmatic products associated with the final phases of the Variscan Orogeny in the late Carboniferous–early Permian of northern Europe is remarkable and indicates some of the complexities involved in melt generation in tectonically active regions of the planet. Similar melt heterogeneity can be seen in the early sequences of many large continental flood basalt provinces including the Paraná-Etendeka Igneous Province (Peate 1997). To explain the diversity of Carboniferous–Permian magmatism we advocate variable degrees of melting at different depths from sources that have been enriched by either metasomatism or subduction-related processes across northern Europe. Crustal assimilation/contamination and high level fractionation are also important processes, but a key outstanding question is why such source variability is seen.

From the considerable variation in Sm/Yb ratios it is evident that one aspect of this complexity is the thickness of the lithosphere. On average, melt generation will occur at greater depths (garnet stability field, >75 km, Nickel 1986) in areas underlying a thick lithosphere and at shallower depths (spinel stability field) when the lithospheric is thinner. From recent geophysical surveys it is evident that magmatism across the different regions from Scotland to Sweden was erupted through crust of highly variable composition and thickness. Lithospheric thickness varies from Laurentia (<80 km, Scotland) to Baltica (>100 km, Norway and Sweden) (Pascal et al. 2004). However, particular areas such as Scania in southern Sweden and the Oslo Graben suffered major amounts of attenuation during the Carboniferous–Permian (Wilson et al. 2004) with the result that melt-production potentially occurred at variable depths. This lithospheric attenuation may explain why in this investigation we have shown that the melts produced over the greatest range of depth were formed in Scotland (Sm/Yb ~ 5, garnet stability field) where the lithosphere was apparently thinner initially, rather than in Sweden or Norway where the overall lithospheric thickness was greater at the beginning of the Carboniferous.

Not all the dykes were emplaced as rapidly as those containing mantle xenoliths from Scotland, and high level fractional crystallisation, accumulations of phenocrysts in the magma chamber, melt separation and crustal contamination, were important processes in modifying the melt composition. The porphyritic nature and broad compositional range of the intrusions indicates magma residence in crustal magma chambers. This conclusion is also supported by geophysical investigations that show high seismic velocities in the lower crust ascribed to basaltic underplating (Neumann et al. 1988, 2004 and references therein). Liquid-crystal segregation took place during emplacement of the intrusions as well as in magma chambers. The complexity of pyroxene zonation and trapped melt inclusions further indicate a polybaric fractionation history, with pyroxene crystallisation having commenced at pressures up to 1.15 GPa (Kirstein et al. 2002). A number of the alkaline dykes from Scotland, particularly those containing garnet-bearing mantle xenoliths, originated as small melt fractions (~3%) from an enriched source in the garnet stability field. The remaining sills also retain evidence of garnet being present in their source region, but represent higher degree melts (<10%) and have had greater interaction with the lithosphere and crust.

The lithosphere beneath northern Europe is undoubtedly chemically heterogeneous with 'thin spots' and 'thick spots' depending on the previous tectonic history (Fig. 12). These 'spots' are potentially transient and could melt at different times and produce different melt types. Part of the variation in the melt composition may be due to lithospheric erosion due to melting of readily fusible domains or 'wet spots'. Consequently it

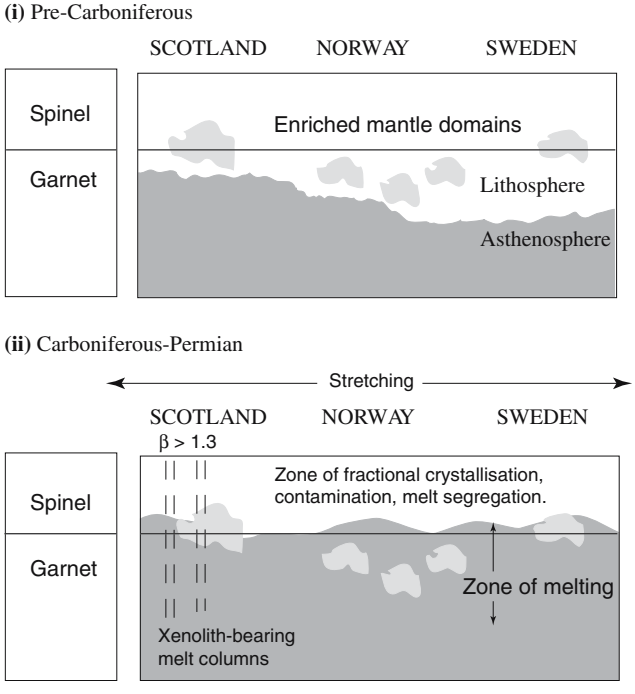

Fig. 12 Schematic diagram (not to scale) of (*i*) mantle prior to Carboniferous–Permian melting and (*ii*) during melting. Stretching factor (β) for Scotland after Smith et al. (1999). Lithospheric thickness variation after Pascal et al. (2004)

is not surprising that the role of volatiles in the genesis of the alkaline samples appears extremely important. Melt generation within the lithospheric mantle is facilitated by the presence of just 0.3 wt% $CO_2 \pm H_2O$, which allows melting to occur at the lower temperature, volatile-present solidus (Gallagher and Hawkesworth 1992). The presence of volatile-rich accessory phases (including apatite and fluorite), as well as hydroxyl ion bearing minerals (amphibole and biotite) in the dyke and sill intrusions of Norway indicates that volatiles were abundant. Amphibole also occurs in intrusions in Scotland and Sweden. Modelling of melting by inversion of rare earth elements in basaltic lavas from the Firth of Forth area, Scotland by Smith et al. (1999) led to the conclusion that moderate lithospheric stretching ($\beta \geq 1.3$) would be sufficient to decompress and melt the source region.

The present study establishes that the alkaline minor intrusions from Norway contain a significant lithospheric component. Neumann et al. (2004) also concluded that the lithospheric mantle was a major component in the generation of the basaltic magmatism of the Oslo Graben. The larger degrees of melting and generally less trace element-enriched source of the cross-cutting suite of tholeiitic dykes suggests that extension led to melting of volatile-bearing lithosphere and that continued extension left the way open for decompression melting of the asthenosphere and formation of the later tholeiites. The small volume of tholeiites sampled in this study and recorded by previous workers (e.g. Neumann et al. 2004) can readily be explained by decompression melting of the underlying asthenosphere in response to localised lithospheric extension (Fig. 12). Together these data provide no evidence for a thermal anomaly beneath Norway. Coupled with the contemporaneous nature of tholeiitic magmatism across northern Europe we can find no evidence of the involvement of a mantle plume in the genesis of the Carboniferous–Permian magmatism that is widespread across northern Europe. This conclusion is at odd with the plume model proposed by Ernst and Buchan (1997), who used the inferred intersection of dyke swarms to advocate the presence a mantle plume under the North Sea. It is widely acknowledged that planes of weakness in the crust probably controlled local magmatism (e.g. Upton et al. 2004) and so the apparent dyke orientation may be a relic of larger tectonic features. In Scotland Carboniferous–Permian dykes are emplaced sub-parallel to the NE–SW and ENE–WSW Caledonian trend and/or the coeval extensional structures. In Norway dyke emplacement is sub-parallel to terrane boundaries in the Pre-Cambrian basement (Andersen et al. 2002).

Rapid vertical melt transport is inferred by the presence of numerous mantle xenoliths in the alkaline dykes of Scotland (Upton et al. 1983). Mantle xenoliths have not been found elsewhere, which suggests that either the crust was thicker and less fractured or the magmas less volatile-rich. Geophysical surveys and palinspastic reconstructions suggest that the crust in Scotland was thinner than in Scandinavia (see Pascal et al. 2004), which leads us to suggest that crustal thickness and pre-existing weaknesses were important parameters in focussing both the locus and depth of melt generation (Fig. 12). Melting of the lithosphere strongly implies that volatiles were important in all regions for melt generation. This may potentially be related to the positioning of these locations relative to the Variscan orogenic front and ancient subduction margins, but is more likely to be related to the observed metasomatic enrichment of the British and Scandinavian mantle by carbonatitic fluids (Menzies and Halliday 1988; Neumann et al. 2004). Pre-existing lithospheric heterogeneity would only have been amplified by the closure of the Rhenohercynian Ocean prior to Variscan orogenesis increasing the possibility of local melt generation (Fig. 12).

Conclusions

1. Regional differences between the tholeiitic and alkaline minor intrusions highlight the heterogeneous nature of the mantle underlying northern Europe during the Carboniferous–Permian.
2. The source of the tholeiite intrusions is similar to E-MORB but the majority of the samples have been contaminated by lithospheric melts and continental crust with high Th and low Nb/La.
3. The tholeiites have high $(Tb/Yb)_N$ ratios indicative of melting at depth in the presence of residual garnet. Tholeiites from Scotland have higher $(Tb/Yb)_N$ ratios than those from Sweden and Norway and formed at greater depths despite apparently being formed beneath a thinner overlying lithosphere.
4. Tholeiites from the Oslo Graben section have undergone the least interaction with lithospheric mantle, presumably because the lithosphere in this region had been thinned considerably during extension prior to their formation.
5. The largest sample diversity occurs in Norway, where mafic to felsic alkaline intrusions occur together with sub-alkaline tholeiites. The first melts were produced in a volatile-rich environment ascribed to melting of metasomatised lithosphere.

6. Alkali basalts were produced by variable degrees of melting of a garnet-rich asthenospheric source followed by mixing with lithosphere derived melts, some derived from within the spinel stability field.
7. This work provides no evidence for a thermally anomalous mantle plume during Carboniferous–Permian magmatism in northern Europe.

Acknowledgments We gratefully acknowledge funding during this work by the European Commission TMR Network project ''Permo–Carboniferous rifting in Europe'' (ERB-FMRXCT960093). The input of all the network partners is appreciated in discussing ideas relating to this work. The assistance of Prof. Terry Plank, Boston University and Dr. Pieter Vroon, Vrije Universiteit in the production of data is appreciated. Acknowledgement of this funding source and co-workers does not imply that they concur with the conclusions drawn herein. Reviews by Alison Monaghan and E-R Neumann were appreciated and substantially improved the original manuscript. We are also indebted to Ian Parsons for his editorial contributions.

Appendix 1

Appendix 2: Analytical methods

Major- and trace-element analyses

Sample crushing was carried out in a steel jaw crusher. 100 g of the crushate was milled in an agate ball mill at the Vrije Universiteit, Amsterdam. Glass beads for major element analyses and powder pellets for trace elements were then prepared and analysed using a Philips PW1404/10 X-ray fluorescence spectrometer with a Rh-anode X-ray tube. For further details on XRF analyses at the Vrije Universiteit see Heumann and Davies (1997).

ICP-MS analyses

Samples were analysed on a VG PlasmaQuad ExCell ICP-MS at the Department of Earth Sciences at Boston University. Instrument backgrounds are <0.5 cps. Routine precision is 1–2% RSD for most trace element to <20 ppb in the rock. Sample (0.05 g)

Table 4 Additional major and trace element data for tholeiitic and alkalic samples analysed by XRF

Sample	Country	Type	SiO_2	TiO_2	Al_2O_3	Fe_2O_3	MnO	MgO	CaO	Na_2O	K_2O	P_2O_5	LOI	Total	Rb	Sr	Y	Zr	Nb	V	Ni
WR-1	Scotland	Dyke	48.22	2.54	13.35	13.86	0.16	4.70	9.33	2.59	0.89	0.28	3.47	99.4	20	344	30	167	17	367	41
Knock1	Scotland	Dyke	47.69	2.45	13.92	14.46	0.14	4.64	6.79	3.26	0.57	0.32	5.60	99.8	15	399	33	196	18	392	51
AU-1	Scotland	Dyke	50.13	2.34	13.70	13.37	0.22	6.28	7.26	2.70	1.68	0.29	2.00	100.0	30	364	30	171	17	352	53
LH-1	Scotland	Dyke	50.30	2.04	14.00	12.49	0.19	6.40	10.15	2.22	0.47	0.18	1.30	99.7	8	286	27	151	15	322	107
AD-1	Scotland	Sill	46.40	2.41	13.80	15.43	0.16	4.72	5.89	3.17	0.37	0.31	7.40	100.1	9	116	30	184	18	402	48
BRQ-1	Scotland	Sill	47.90	2.94	12.70	16.52	0.21	5.22	9.17	2.57	0.69	0.28	1.50	99.7	18	341	30	169	16	562	47
TL-1	Scotland	Sill	50.10	2.31	13.60	13.72	0.16	5.60	7.37	3.03	1.61	0.30	2.00	99.7	21	389	28	160	16	449	50
Croy-1	Scotland	Sill	50.20	2.18	14.10	12.80	0.17	5.57	9.06	2.89	1.16	0.26	1.50	99.8	32	443	28	161	15	313	57
BRQ-2	Scotland	Sill	50.90	2.95	12.80	14.70	0.21	4.21	6.58	3.37	1.46	0.39	1.70	99.3	39	332	39	238	22	328	71
Bil-3	Sweden	Sill	48.85	1.79	15.19	12.82	0.17	7.48	9.84	2.61	0.44	0.16	0.27	99.6	9	345	21	80	8	NA	NA
Kin-1	Sweden	Sill	49.31	1.97	14.75	13.32	0.18	6.76	9.89	2.63	0.50	0.18	0.54	100.0	10	370	24	100	10	285	73
StC-1	Scotland	Dyke	39.08	2.83	12.32	12.33	0.18	9.16	11.84	1.28	2.68	0.93	6.00	98.8	78	1135	26	283	100	251	173
Moy-3	Scotland	Dyke	42.21	2.70	11.53	11.99	0.16	8.00	9.20	2.27	2.05	0.59	7.80	98.6	45	837	24	321	55	220	261
C-1	Scotland	Sill	47.70	1.99	14.60	11.55	0.17	8.10	8.93	3.34	1.12	0.45	2.30	100.3	24	495	25	159	44	189	131
BS-7	Sweden	Sill	46.05	4.10	14.35	15.16	0.21	5.22	6.05	3.26	2.57	0.56	2.00	99.5	63	686	36	272	35	318	31
HvS-1	Sweden	Sill	51.76	2.51	15.85	10.34	0.16	3.40	6.04	4.12	2.90	0.64	1.20	99.0	94	588	48	581	96	220	36
VB-2	Sweden	Sill	52.03	2.51	16.05	10.34	0.16	3.41	6.16	4.16	2.79	0.64	1.20	99.5	91	573	48	584	98	218	36
Os-6	Norway	Dyke	44.58	4.22	14.90	15.66	0.20	4.74	8.48	2.80	1.28	0.59	1.50	99.0	54	606	37	285	36	311	31
Bile-3	Norway	Dyke	44.66	2.78	13.24	14.09	0.21	7.20	9.76	2.34	1.20	0.44	3.50	99.5	20	820	28	267	46	371	90
Vo-2	Norway	Dyke	46.50	2.51	15.41	10.77	0.20	4.87	7.60	3.23	2.13	1.05	4.80	99.2	43	1541	24	200	64	203	31
Vo-3	Norway	Dyke	46.65	2.38	15.41	10.06	0.18	4.20	7.42	3.35	2.21	1.05	4.50	97.5	46	1532	25	212	67	193	28
BSd-2	Norway	Dyke	47.21	2.18	16.06	9.88	0.21	3.72	5.83	5.24	1.98	1.46	5.20	99.1	46	1035	43	375	77	87	4
Hov-14	Norway	Dyke	47.83	2.50	15.05	10.76	0.21	3.97	6.16	4.59	1.73	1.75	4.30	99.0	32	1052	44	329	71	114	4
KK-3	Norway	Dyke	49.02	2.15	16.25	9.23	0.14	4.13	5.23	5.23	1.39	0.90	5.80	99.6	33	1287	34	400	91	188	3
NH-15	Norway	Dyke	49.46	1.95	16.79	8.47	0.13	3.16	4.79	4.27	1.81	0.59	7.60	99.1	53	406	38	326	73	178	4
M10	Norway	Sill	55.48	1.95	13.68	11.67	0.21	1.87	4.84	3.67	3.30	0.79	1.90	99.4	114	300	88	821	94	44	5
Li14	Norway	Sill	57.89	1.28	16.08	6.24	0.20	1.28	2.38	5.18	5.40	0.42	1.60	98.2	128	370	63	961	188	26	5
KK-1	Norway	Sill	56.09	1.77	16.67	7.98	0.22	1.53	3.35	5.23	4.92	0.66	0.60	99.1	145	431	61	985	196	49	5
Li15	Norway	Sill	66.41	0.57	15.28	3.37	0.15	0.38	0.47	5.34	4.70	0.03	1.00	97.7	114	49	110	1765	352	8	1
Hov-11	Norway	Sill	69.14	0.27	15.18	3.09	0.27	0.18	0.02	5.78	5.04	0.02	0.30	99.3	157	12	120	1512	335	10	1

Estimated relative accuracy due to calibration errors ± 1%. Total Fe as Fe_2O_3

Dashed line indicates division between tholeiitic and alkalic samples

NA not analysed

was digested using HNO3 and HF acids. Once dissolved the sample was dried and then re-dissolved in HNO_3 and distilled H_2O. The solution was tranfered to a Nalgene bottle and sonicated for 30 min. Finally the sample was diluted further prior to running in the ICPMS. Standards run with the samples included W-2, BHVO-1 and JB-3.

Appendix 3

Table 5 Locations and co-ordinates of samples in data tables

	X	*Y*	Location
Scotland[a]			
DCW-1	366308	6252422	Dalcruie Weir
MdC-1	459677	6281279	Milton of Dalcappon, Pitlochry
LC-1	460654	6200297	Lochcote Reservoir, Linlithgow
PW-1	463811	6223942	Powmill Quarry, Powmill
LC-3	459756	6200184	Lochcote Reservoir, Linlithgow
ARN-1	483152	6228022	Auchmuirbridge, Glenrothes
Stc-4	355860	6310658	Streap Comhlaidh, Fort William
A7ii	369254	6304056	Allt Dogha, Fort William
Moy-5	377482	6308875	Allt Coire Chraoibhe, Fort William
NB-1	516969	6213113	North Berwick
Hh-1	397549	6159540	Hillhouse Quarry, Irvine
CK-1	406515	6140921	Craigs of Kyle Quarry, Ayr
Sweden[b]			
AL-1	287692	6472710	Slävik, Bohuslän
HV-1	282186	6490140	Valön, Bohuslän
HV-2	282186	6490140	Valön, Bohuslän
VB-2	279606	6521590	Västbacka, Bohuslän
HVS-1	280649	6517800	Havstensund, Bohuslän
M-1	345228	6240050[c]	Mölle, Scania
ML-1	344703	6241120	Paradishamn, Scania
D-2	398419	6168690	Dalby, Scania
TK-1	416481	6171200	Torpa Klint, Scania
BIL-1	427986	6462900	Billingen, Västergotland
Oslo[d]			
Li-11	592900	6640200	Lindøya, Oslo
Vo-1	602700	6645950	Vollebæk, Oslo
GR-12	596005	6639300	Gressholmen, Oslo
NH-13	594850	6640100	Nakholmen, Oslo
HOV-13	597200	6640800	Hovedøya, Oslo
FBU-1	589570	6639320	Fornebu, Oslo
Bile-2	592250	6598000	Bile Island, Oslofjord
OS-2	587525	6637575	Ostøya, Bærum
OS-5	587625	6636950	Ostøya, Bærum
Li-13	595950	6640150	Lindøya, Oslo
HG-1	595900	6639850	Gressholmen, Oslo
SL-1	584650	6639000	Slependen, Bærum
Vo-4	602700	6645950	Vollebæk, Oslo
HUS-2	592800	6645450	Husebyeåsen, Oslo
VK-1	555700	6646850	Vikersund
JN-1	586250	6694300	Jaren
Hy-1	485650	6478850	Hisøy
Hy-2	486050	6476450	Hisøy
Hy-4	489400	6482000	Arendal
KB-1	533750	6611650	Kongens Gruve, Kongsberg[e]

[a] Projection: UTM Zone 30; Datum: ETRS89

[b] Projection: UTM Zone 33; Datum: ED50

[c] Approximate position; Projection: UTM Zone 33, Datum WGS84

[d] Projection: UTM Zone 32; Datum: WGS84

[e] Main shaft of the mine; Datum: ED50

References

Andersen T, Knudsen T-L (2000) Crustal contaminants in the Permian Oslo Graben, South Norway; constraints from Precambrian geochemistry. Lithos 53:247–264

Andersen T, Griffin WL, Pearson NJ (2002) Crustal evolution in the SW part of the Baltic Shield: the Hf isotope evidence. J Petrol 43:1725–1747

Baxter AN, Mitchell JG (1984) Camptonite-monchiquite dyke swarms of northern Scotland; age relationships and their implications. Scott J Geol 20:297–308

Bylund G, Johansson L, Johansson I, Solyom Z, Nilsson M, Rhode A Gorbatschev R (1988) Mafic dyke swarms of southernmost Sweden –40 S. In: Excursion guide International symposium on mafic dykes and magmatism in rifting and intraplate environments, Lund

Corfield SM, Gawthorpe RL, Gage M, Fraser AJ, Besly BM (1996) Inversion tectonics of the Variscan foreland of the British Isles. J Geol Soc Lond 153:17–32

Dahlgren S, Corfu F, Heaman LM (1996) U–Pb isotopic time constraints, and Hf and Pb source characteristics of the Larvik plutonic complex, Oslo Paleorift. In: Geodynamical and geochemical implications for the rift evolution, V.M. Goldschmidt Conference, Ruprecht-Karls Universität, Heidelberg, Germany, pp120

DeSouza HAF (1982) Age data from Scotland and the Carboniferous time scale. In: Odin GS (eds) Numerical dating in stratigraphy. Wiley, London, pp 455–465

Ellam RM (1992) Lithospheric thickness as a control on basalt geochemistry. Geology 20:153–156

Ernst RE, Buchan K (1997) Giant radiating dyke swarms; their use in identifying pre-Mesozoic large igneous provinces and mantle plumes. In: Mahoney JJ, Coffin MF (eds) Large igneous provinces; continental, oceanic, and planetary flood volcanism. American Geophysical Union, pp 297–333

Francis EH (1991) Carboniferous–Permian igneous rocks. In: Craig GY (eds) Geology of Scotland. The Geological Society, London, pp 393–420

Gallagher K, Hawkesworth CJ (1992) Dehydration melting and the generation of continental flood basalts. Nature 358:57–59

Glennie KW (1998) Lower Permian-Rotliegend. In: Glennie KW (eds) Petroleum geology of the North Sea: basic concepts and recent advances. Blackwell, Oxford, 137–173

Govindaraju K (1994) Compilation of working values and sample description for 383 geostandards. Geostand Newslett 18:1–158

Heumann A, Davies GR (1997) Isotopic and chemical evolution of the post-caldera rhyolitic system at Long Valley, California. J Petrol 38:1661–1678

Kirstein LA, Peate DW, Hawkesworth CJ, Turner S, Harris C, Mantovani M (2000) Early Cretaceous basaltic and rhyolitic magmatism in southern Uruguay associated with the opening of the South Atlantic. Jour Petrol 41(9):1413–1438

Kirstein LA, Hawkesworth CJ, Garland FE (2001) Silicic lavas or rheomorphic ignimbrites? a chemical distinction. Contrib Mineral Petrol 142:309–322

Kirstein LA, Dunworth EA, Nikogosian IK, Touret JLR, Lustenhouwer WJ (2002) Initiation of melting beneath the Oslo Graben: a melt inclusion perspective. Chem Geol 183:121–236

Klingspor I (1976) Radiometric age determination of basalts, dolerites and related syenite in Skane, southern Sweden. Geol Fören Stock Förhand 98:195–216

Kresten PS, Samuelsson L, Rex D (1981) Ultramafic dykes of the northern Skagerrak coast of Sweden. Geol Fören Stock Förhand 103:285–289

Larsen LM, Pedersen AK, Sundvoll B, Frei R (2003) Alkali picrites formed by melting of old metasomatized lithospheric mantle: Manîtdlat Member, Vaigat Formation Palaeocene of west Greenland. J Petrol 44:33–38

Leeder M (1982) Upper Palaeozoic basins of the British Isles—Caledonide inheritance versus Hercynian plate margin processes. J Geol Soc Lond 139:479–491

Le Maitre RW, Bateman P, Dudek A, Keller J, Le Bas MJ, Sabine MA, Schmid R, Sorensen H, Streckeisen A, Wooley AR, Zanetlin B (1989) A classification of igneous rocks and glossary of terms. Blackwell, Oxford

Løvlie R, Mitchell JG (1982) Complete remagnetization of some Permian dykes from western Norway induced during burial/uplift. Phys Earth Planet Int 30:415–421

MacDonald R, Gottfried D, Farrington MJ, Brown FW, Skinner NG (1981) Geochemistry of a continental tholeiite suite: late Palaeozoic quartz dolerite dykes of Scotland. Trans R Soc Edin (Earth Sci) 72:57–74

Maynard JR, Hofmann W, Dunay RE, Bentham PN, Dean KP, Watson I (1997) The Carboniferous of western Europe: the development of a petroleum system. Petrol Geosci 3:97–115

Menzies M, Halliday A (1988) Lithospheric mantle domains beneath the Archean and Proterozoic crust of Scotland, J Petrol Spec Lithos Iss 175–302

McCann T (1999) The tectonosedimentary evolution of the northern margin of the Carboniferous foreland basin of NE Germany. Tectonophysics 313:119–144

Monaghan A, Pringle M (2004) High precision 40-Ar/39-Ar geochronology of the Permo-Carboniferous volcanism in the Midland Valley, Scotland. In: Wilson M, Neumann E-R, Davies GR, Timmerman MJ, Heeremans M, Larsen B (eds) Permo-Carboniferous magmatism and rifting in Europe. Geological Society, London, Special Publication, vol 223, pp 219–242

Neumann E-R, Tilton GR, Tuen E (1988), Sr, Nd and Pb isotope geochemistry of the Oslo rift igneous province, southeast Norway. Geochim Cosmochim Acta 52:1997–2007

Neumann E-R, Olsen KH, Baldridge WS, Sundvoll B (1992) The Oslo Graben: a review. Tectonophysics 208:1–18

Neumann E-R, Wilson M, Heeremans M, Dunworth E-A, Obst K, Timmerman MJ, Kirstein LA (2004) Carboniferous–Permian rifting and magmatism in southern Scandinavia, the North Sea and northern Germany: a review. In: Wilson M, Neumann E-R, Davies GR, Timmerman MJ, Heeremans M, Larsen B (eds) Permo-Carboniferous magmatism and rifting in Europe. Geological Society, London Special Publication vol 223, pp11–40

Nickel KG (1986) Phase equilibria in the system SiO_2–MgO–Al_2O_3–CaO–Cr_2O_3 (SMACCr) and their bearing on spinel/garnet lherzolite relationships. Neues Jahr Min Abhand 155:259–287

Niu Y, O'Hara MJ (2003) Origin of ocean island basalts: a new perspective from petrology, geochemistry, and mineral physics considerations. J Geophys Res 108:10.1029/2002JB002048

Obst K, Solyom Z, Johansson L (2004) Permo-Carboniferous extension-related magmatism at the southwestern margin of the Fennoscandian Shield. In: Wilson M, Neumann E-R, Davies GR, Timmerman MJ, Heeremans M, Larsen B (eds) Permo-Carboniferous magmatism and rifting in Europe. Geological Society, London Special Publication vol 223, pp 259–288

Pascal C, Cloetingh SAP, Davies GR (2004) Asymmetric lithosphere as the cause of rifting and magmatism in the Permo-Carboniferous Oslo Graben. In: Wilson M, Neumann E-R, Davies GR, Timmerman MJ, Heeremans M, Larsen B (eds) Permo-Carboniferous magmatism and rifting in Europe. Geological Society, London Special Publication, vol 223, pp 139–156

Peate DW (1997) The Paraná-Etendeka Province. In: Mahoney JJ, Coffin MF (eds) Large igneous provinces: continental, oceanic, and planetary flood volcanism. American Geophysical Union, Washington pp 217–245

Pederson LE, Heaman LM, Holm PM (1995) Further constraints on the thermal evolution of the Oslo Graben from precise U–Pb zircon dating in the Siljan-Skrim area. Lithos 34:301–315

Ramberg IB, Larsen BT (1978) Tectonomagmatic evolution. In: Dons JA, Larsen BT (eds) The Oslo palaeorift: a review and guide to excursions. Norsk Geol Unders pp 55–73

Rock NM (1983) The Permo-Carboniferous camptonite-monchiquite dyke suite of the Scottish Highlands and islands: distribution, field and petrologic aspects. 82/14: Report of the Institute of Geological Sciences

Rollinson H (1993) Using geochemical data: evaluation, presentation, interpretation. Longman, England, p 352

Samuelsson L (1971) The relationship between Permian dikes of dolerite and rhomb porphyry along the Swedish Skagerrak coast. Sver Geol Under 65(9):3–51

Scott PW, Middleton R (1983) Camptonite and Maenaite sills near Gran Hadeland, Oslo Region. Norsk Geologiske Unders 389:1–26

Smedley P (1988) Trace element and isotopic variations in Scottish and Irish Dinantian volcanism: evidence for an OIB-like mantle source. J Petrol 29:413–443

Smith PM, Gibson SA, McKenzie DP, Thompson RN, White NJ (1999) Quantifying the relationship between Permo-Carboniferous magmatism and extension in Scotland. J Conf Abs 4:293

Smythe DK (1994) Geophysical evidence for ultrawide dykes of the late Carboniferous quartz-dolerite swarm of northern Britain. Geophys J Int 119:20–30

Sun S, Mc Donough WF (1989) Chemical and isotopic systematics of oceanic basalts: Implications for mantle composition and processes. In: Saunders AD, Norry MJ (eds) Magmatism in the ocean basins. Geological Society Special Publication, London pp 313–345

Sundvoll B, Neumann E-R, Larsen BT, Tuen E (1990) Age relations among Oslo Graben magmatic rocks: implications for tectonic and magmatic modelling. Tectonophysics 178:67–87

Taylor SR, McLennan SM (1985) The continental crust: its composition and evolution. Blackwell, Oxford

Timmerman MJ (2004) Timing, geodynamic setting and character of Permo-Carboniferous magmatism in the foreland of the Variscan Orogen, NW Europe. In Wilson M, Neumann E-R, Davies GR, Timmerman MJ, Heeremans M, Larsen B (eds) Permo-Carboniferous magmatism and rifting in Europe. Geological Society, London Special Publication, vol 223, pp 41–74

Tomkeieff SI (1937) Petrochemistry of the Scottish Carboniferous-Permian igneous rocks. Bull Volcan 1:59–87

Upton BGJ, Aspen P, Chapman NA (1983) The upper mantle and deep crust beneath the British Isles: evidence from inclusions in volcanic rocks. J Geol Soc Lond 140:105–122

Upton BGJ, Stephenson D, Smedley PM, Wallis SM, Fitton JG (2004) Carboniferous and Permian magmatism in Scotland. In: Wilson M, Neumann E-R, Davies GR, Timmerman MJ, Heeremans M, Larsen B (eds) Permo-Carboniferous magmatism and rifting in Europe. Geological Society, London Special Publication, vol 223, pp 195–218

Walker F (1935) The late Palaeozoic quartz dolerites and tholeiites of Scotland. Min Mag 24:131–159

Wallis SM (1989) Petrology and geochemistry of upper Carboniferous: lower Permian volcanic rocks in Scotland. Unpublished PhD thesis, University of Edinburgh

Wilson M, Neumann E-R, Davies GR, Timmermann MJ, Heeremans M, Larsen BT (2004) Permo-Carboniferous magmatism and rifting in Europe-an introduction. In: Wilson M, Neumann E-R, Davies GR, Timmermann, MJ, Heeremans M, Larsen BT (eds) Permo-Carboniferous magmatism and rifting in Europe. Geological Society, London Special Publication, vol 223, pp 1–10

Winchester JA, Floyd PA (1977) Geochemical discrimination of different magma series and their differentiation products using immobile elements. Chem Geol 20:325–343

Wood DA, Tarney J, Varet J, Saunders AD, Bougault H, Joron JL, Treuil M, Cann JR (1979) Geochemistry of basalts drilled in the North Atlantic by IPOD Leg 49: implications for mantle heterogeneity. Earth Planet Sci Lett 42:77–97

Wooden JL, Czamanske GK, Fedorenko VA, Arndt NT, Chauvel C, Bouse RM, King B-S, Knight RJ, Siems DF (1993) Isotopic and trace-element constraints on mantle and crustal contributions to Siberian continental flood basalts, Noril'sk area, Siberia. Geochim Cosmochim Acta 57:3677–3704

Ziegler PA (1990) Geological atlas of Western and Central Europe. Shell International Petroleum Maatschappij BV, Geological Society, Bath, 240pp

Zindler A, Hart SR (1986) Chemical geodynamics. Annu Rev Earth Planet Sci 14:493–571